Quaternary Research
Copyright © University of Washington. Published by Cambridge University Press, 2020.
doi:10.1017/qua.2020.22

Holocene hydroclimatic variability in the Zanskar Valley, Northwestern Himalaya, India

Sheikh Nawaz Ali[a]*, Shailesh Agrawal[a], Anupam Sharma[a], Binita Phartiyal[a], Paulramasamy Morthekai[a], Pawan Govil[a], Ravi Bhushan[b], Shazi Farooqui[a], Partha Sarathi Jena[b], Ajay Shivam[b]

[a]Birbal Sahni Institute of Palaeosciences, Lucknow, India
[b]Physical Research Laboratory, Ahmadabad, India
*Corresponding author at: snawazali@gmail.com

(Received November 11, 2019; Accepted March 3, 2020)

Abstract

A 1.3-m-long sediment core from the Penzi-la pass, Zanskar Valley, provides a record of hydroclimatic conditions and abrupt climate changes over short time scales since the mid-Holocene. These climatic changes of centennial time scale are crucial to understanding the hydroclimatic variability in northwestern (NW) Himalaya. Relatively higher $\delta^{13}C$ values complemented by total organic carbon, loss on ignition, grain size parameters, and lower Rubidium/Strontium ratios during the Late Northgrippian imply that the area had a dry climate during the period from ~6200–4500 cal yr BP. Subsequently, a relatively stable hydroclimatic environment was experienced between ~4500 and 3400 cal yr BP. After ~3400 cal yr BP the multiproxy data show gradual strengthening of hydroclimatic conditions, however, this trend is interrupted by high-amplitude abrupt reversals (dry events) with a stepwise decreasing intensity at ~3300, 2600, 1700, and 400 cal yr BP. The two most important climatic events of the last millennia (i.e., Medieval Climate Anomaly and the Little Ice Age) were also recorded from the sedimentary archive. Overall, our data show a progressive increase in the moisture availability in the Zanskar Valley and are in agreement with the late Holocene climatic trends of central and western Himalaya.

Keywords: Stable carbon isotope; Grain-size; Rb/Sr ratio; Medieval climate anomaly; Little ice age; Zanskar Valley

INTRODUCTION

The last ~6000 years of the Earth's climate history has not seen high-amplitude climate change events (stable boundary condition; Petit et al., 1999; Warner et al., 2008); however, the lower amplitude changes in the Indian summer monsoon (ISM) and the smaller and short-lived climatic events such as the one at 4.2 kyr BP have proven to have drastic effects on human civilizations such as the expansion and de-urbanization of the Indus Valley (Harappan) civilization, the rise and fall of the Vedic civilization, and the collapse of the Tibetan Guge Kingdom (Witzel, 1987, 1999; Ratnagar, 2002;Staubwasser et al., 2003; Kulke and Rothermund, 2004; Yuan, 2009; Wright, 2010; Giosan et al., 2012; Dixit et al., 2014; Sarkar et al., 2015; Kathayat et al., 2017; Petrie et al., 2017; Misra et al., 2019). The Holocene period has experienced both long- and short-term climate events including the Holocene Climate Optimum, the 8.2 and 4.2 ka climate events, the Medieval Climate Anomaly (MCA; wetter) and the Little Ice Age (LIA; drier). However, the expressions of these events have not been reported in every study (Staubwasser et al., 2003; Dixit et al., 2014, 2018; Dixit and Tandon, 2016; Bird et al., 2017; Misra et al., 2019). This time frame is of great interest for understanding the forcing factors and responses of earth's climate with abundant paleoclimatic proxy records that can be validated through global climate model simulations and used for future climate predictions (Overpeck et al., 1996; Gupta et al., 2003; Fleitmann et al., 2007; Warner et al., 2008). To reconstruct the climatic records, precise timing of the paleoclimatic archives and high-resolution proxy data are needed. However, such data from the Indian subcontinent, and more specifically from the Himalayan region, are scanty and often suffer from age uncertainties (Sinha et al., 2007; Prasad, S. et al., 2014; Ghosh et al., 2015; Mishra et al., 2015; Ali et al., 2018; Bhushan et al., 2018; Sharma and Phartiyal, 2018; and references therein). It has been observed that the climate reconstructions from moderate- to high-precipitation areas (rainfall ~1000 mm/yr; central and eastern Himalaya) and extremely low-precipitation areas (e.g., Tso Moriri lake) do

Cite this article: Ali, S. N. *et al* 2020. Holocene hydroclimatic variability in the Zanskar Valley, Northwestern Himalaya, India. *Quaternary Research* 97, 140–156. https://doi.org/10.1017/qua.2020.22

https://doi.org/10.1017/qua.2020.22 Published online by Cambridge University Press

not respond to minor climatic events (shorter duration and smaller magnitude). This has been attributed to the insignificant/irresolvable responses of proxies in wet areas and to the buffering effect of snow melt and weaker late Holocene ISM in dry areas. Moreover, spatial differences in the climate change patterns in the ISM region also exist (Prasad and Enzel, 2006; Sinha et al., 2011; Mishra et al., 2015; Ali et al., 2018). Similarly from marine archives, the identification of climatic events younger than 5000 yr BP is difficult owing to their short duration and low amplitude (Gupta et al., 2003). Hence the transitional climate zones lying between the dry Trans-Himalaya/Tibet area towards the north and the sub-humid Himalaya area towards the south, where the climate signals are amplified, needs to be targeted (Ali et al., 2018).

The Himalayan range extends for ~2500 km in an east–west direction. However, its width is rather variable, rarely exceeding 250 km. This region is influenced by two major weather systems: the ISM (summer) and the mid-latitude westerlies in winter (Finkel et al., 2003; Yang et al., 2008). The influence of these two climate systems varies spatially, and most of the southern and eastern Himalayan ranges receive a moderate-to-heavy summer precipitation from the ISM, while the regions north of the Higher Himalaya and the northwestern (NW) Himalaya receive scanty monsoon precipitation (Ali and Juyal, 2013). Similarly, the influence of the mid-latitude westerlies shows a progressive decrease from the NW (Karakoram and Ladakh) to northeastern Himalaya (Benn and Owen, 1998). As far as the paleoclimatic/paleoenvironmental proxy record of the Higher Himalaya is concerned, the data are rudimentary, especially in relation to the sheer size of this sector; more specifically, the paleoclimatic data from the NW Himalaya are scarce (Ali et al., 2018; Bhushan et al., 2018; Banerji et al., 2020). In the case of the Higher Himalaya, focus must be given to the ISM, as it drives the majority of environmental and ecological changes in the region (Patnaik et al., 2012; Xu et al., 2018). Yet, despite the important role of the ISM in the NW Himalaya, in-depth characterizations of ISM variability prior to the instrumental period are rare, except for a few studies carried out in the far northeast of Ladakh, where the contribution of the ISM is minimal (Wünnemannet al., 2010; Leipe, Demske, Tarasov, 2014; Leipe, Demske, Tarasov, Wünnemann, et al., 2014; Mishra et al., 2015; Dutt et al., 2018). On the basis of these studies, a general trend of aridity is reported from the NW Himalaya for the latter half of the Holocene (Leipe, Demske, and Tarasov, 2014; Mishra et al., 2015). Contrary to this, in the monsoon-dominated central Himalaya, the existing paleoclimatic data suggest fluctuating lake levels throughout the Holocene, and the majority of the records with reasonable chronologies advocate for a gradual intensification of the ISM (punctuated by dry spells) since the mid-Holocene (Rühland et al., 2006; Kotlia and Joshi, 2013; Sanwal et al., 2013; Rawat et al., 2015; Bali et al, 2017; Bhushan et al., 2018; Srivastava et al., 2018). Interestingly, the NW Himalaya (Zanskar, Ladakh) has been and continues to be influenced by both the ISM and the mid-latitude westerlies throughout the late Quaternary (Benn and Owen, 1998; Owen and Dortch, 2014; Mishra et al., 2015; Ganju et al., 2018; Sharma et al., 2018), and recently a water isotope-based study by Sharma and colleagues (2017) reported a significant contribution of ISM precipitation in the upper Indus catchment. However, the hydroclimatic conditions and the geographical extent of the ISM influence in the NW Himalaya is still being debated (Owen and Dortch, 2014). It has also been suggested that the minor changes during the late Holocene have not affected this region because of the early southward migration of the Intertropical Convergence Zone (ITCZ) and/or the attenuating impact of the westerlies and continuing meltwater inflow (Mishra et al., 2015). There is another important factor, the complexity of the Higher Himalayan mountain topography that produces significant variability in the precipitation and rainfall patterns over short distances (Beniston, 2006). Keeping these contradictions and the paucity of data in view, interpretations related to the Holocene climate are still tentative and remain elusive. Hence, multiproxy records must be generated that may reflect local to regional climatic conditions, and they need to be based on robust chronologies (Dearing, 2006; Dearing et al., 2006; Kathayat et al., 2017). Therefore, multiproxy paleoclimatic records covering different sectors of the NW Himalaya are needed for both local as well as regional evaluations of the climate variability during the later parts of the Holocene.

STUDY AREA

The Zanskar Valley (Fig. 1) is located in the transitional zone between the ISM-dominated southern Himalaya and the mid-latitude westerly–dominated northern region. The moisture availability of this valley is regulated by a complex interplay of these two different weather and atmospheric circulation systems (Mayewski et al., 1984; Bothe et al., 2011; Lee et al., 2014; Ali et al., 2018; Sharma and Shukla, 2018). A 17-yr ice-core data set from the Sentik glacier (Nun-Kun; Zanskar Valley), which is located towards the northwestern side of the study area and forms the northern fringe of the Higher Himalaya in the Suru Valley, indicates dominance of the ISM (Mayewski et al., 1984). Because of the dominance of ISM, the Zanskar range receives a relatively higher precipitation (400–600mm/year) than its northern counterparts (Lee et al., 2014; Sharma et al., 2018). Since the Zanskar Valley is located in a climatologically sensitive/critical area, it is expected to provide important insights for understanding temporal changes in the contributions from two climate systems (ISM and westerlies). With these facts in mind, the objectives of the study are (1) to look for low-amplitude climate changes during the late-Holocene, (2) to understand the temporal hydroclimatic variability in the transient climate zone, and (3) to identify the forcing factors responsible for small-scale climatic perturbations.

A sediment core approximately 1.3-m long was collected from a kettle hole lake deposit located at Penzi-la using a PVC pipe (3-inch diameter) that was manually inserted into the ground (33° 52′ 05′ N, 76° 21′ 14′ E; ~4450 m asl;

https://doi.org/10.1017/qua.2020.22 Published online by Cambridge University Press

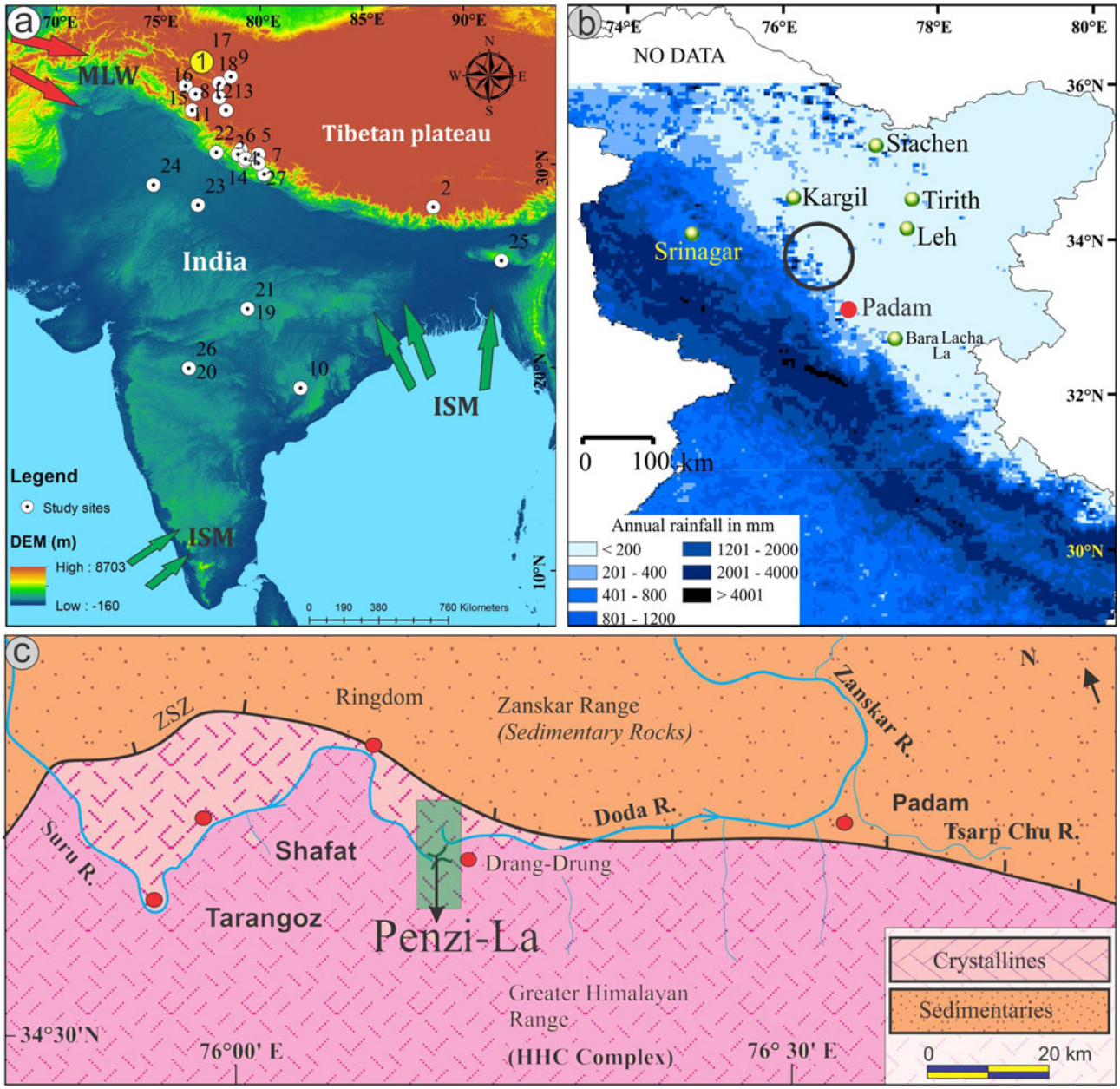

Figure 1. Map compilation. (a) The regional setup of the area along with the trajectories of weather systems—the summer monsoon and the mid-latitude westerlies. The white dots show important terrestrial palaeoclimatic sites that have been discussed in this paper including (1) the Penzi-la (yellow circle; present study), (2) Ali et al., 2018, (3) Bhushan et al., 2018, (4) Srivastava et al., 2018, (5) Rühland et al., 2006, (6) Kotlia and Joshi, 2013, (7) Sanwal et al., 2013, (8) Bali et al., 2017, (9) Rawat et al., 2015, (10) Sinha et al., 2007, (11) Wünnemann et al., 2010, (12) Mishra et al., 2015, (13) Leipe, Demske, and Tarasov, 2014, (14) Kotlia et al., 2015, (15) Sharma et al., 2018, (16) Sharma and Shukla, 2018, (17) Ganju et al., 2018, (18) Lee et al., 2014, (19) Kumar et al., 2019, (20) Sarkar et al., 2015, (21) Kumar et al., 2019, (22) Kathayat et al., 2017, (23) Dixit et al., 2014, (24) Dixit et al., 2018, (25) Dutt et al., 2015, (26) Prasad et al., 2014, and (27) Rühland et al., 2006. (b) The cumulative annual rainfall (mm) map of the western Himalaya (after Juyal, 2014). The circle shows the location of the study site. (c) Geological map of the study area. The Penzi-la (green rectangle) is on the leeward side of the Higher Himalayan Crystallines (HHC) and makes the drainage divide between the Suru and Zanskar Valleys (For interpretation of the references to color in this figure legend, the reader is referred to the web version of this article.)

Figs. 1, 2 and S1). The Penzi-la (a pass between the Suru and Zanskar Valleys) is the gateway to the Zanskar Valley and forms the hydrological divide between the Suru and Doda Rivers at an elevation of ~4500m asl (Figs. 1 and 2, Supplementary Fig. S1). Lithologically, the pass is situated on the rocks of the Higher Himalayan crystalline complex (Fuchs, 1982; Searle and Fryer, 1986). Geomorphologically, the pass represents a typical glacio-fluvial system. Moraine ridges corresponding to different glacial stages are present along the valley floor and sides. The downstream parts also have

https://doi.org/10.1017/qua.2020.22 Published online by Cambridge University Press

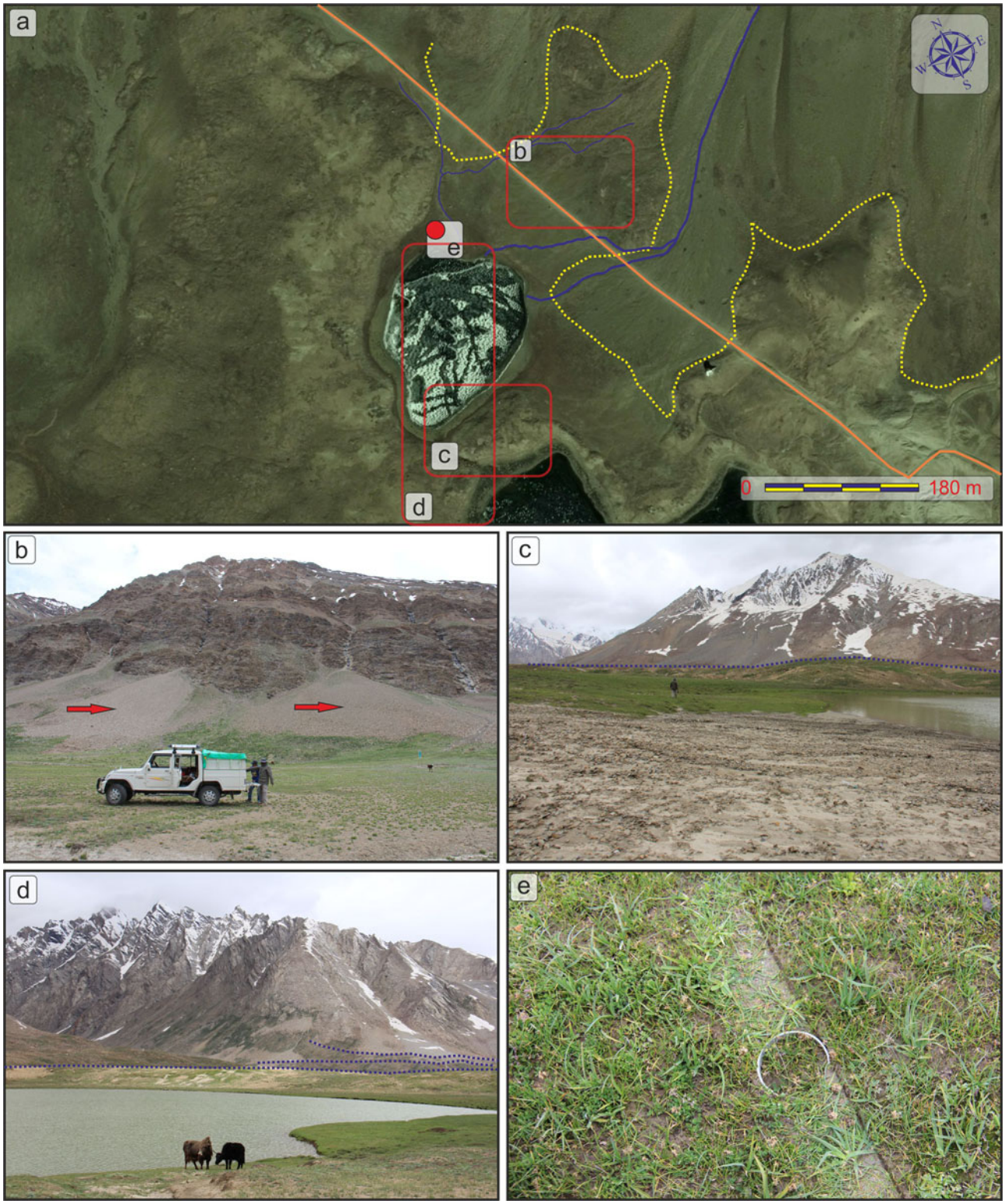

Figure 2. (a) Google Earth imagery showing the boundary of talus cones (yellow dotted line) and the drainages feeding the kettle-hole lake in Penzi-la. Field photographs showing (b) the talus cones (red arrows), (c, d) the lake and the moraine present on the lake boundary (blue dotted line), and (e) the location of the sediment core along the lake boundary as shown in the inset of Figure 2a. (For interpretation of the references to color in this figure legend, the reader is referred to the web version of this article.)

distinctive river terraces. The most prominent features present on the Penzi-la are curvilinear, recessional latero-frontal moraines and kettle hole lakes (Sharma et al., 2018). The kettle hole lakes are depressions formed after the melting of buried ice (in proglacial areas) and have been suggested as important ecological niches in otherwise relatively barren

https://doi.org/10.1017/qua.2020.22 Published online by Cambridge University Press

proglacial environments (Maizels, 1977; Robinson, 2010). These small lakes provide important information on the past geomorphological, sedimentological, and hydrological processes. Hence, the sediment core studied here was placed along the margin of one of the kettle hole lake located towards the north-northwest side of the Penzi-la. Field observations and geomorphology suggest that this small lake is being fed by the runoff (snow melt and rain) from the northeast slopes of the Zanskar Range (Fig. 2, Supplementary Fig. S1).

METHODOLOGY

Different climate proxies have different strengths, weaknesses, and responses in a spatio-temporal context including sensitivity to different forcing factors and time-lag effects; hence, multiproxy studies are desirable (Smol, 2002; National Research Council, 2005; Birks and Birks, 2006). Therefore, in order to reconstruct the hydroclimatic variability in the Zanskar Valley, a sediment core from a kettle hole lake deposit was collected for multiproxy studies. In all, 64 samples (each representing 2 cm of the sediment core) were collected from this core. The samples were analyzed for carbon isotope signature ($\delta^{13}C$) preserved in sediment organic matter (a proxy for past climate changes via paleovegetation and paleoclimate; Cerling, 1992; Ekart et al., 1999), elemental analyses using the Rubidium/Strontium (Rb/Sr) ratio (a proxy for weathering and erosion; Chen et al., 1996, 1999; Jin et al., 2006), and sediment texture/grain size (a proxy for environment and energy conditions; Warrier et al., 2016).

For the analysis of stable carbon isotope ratios of sedimentary organic matter ($\delta^{13}C_{org}$), ~1 g of the sediment sample was taken after coning and quartering and used for decarbonation. Samples were decarbonised with HCl (5%) for 1 hour in a water bath at 50°C; this process was repeated three times. Subsequently, the samples were centrifuged, rinsed repeatedly with deionized water until neutral pH was achieved, and dried. The sample preparation procedures are discussed in detail in Agrawal et al. (2012), Dubey et al. (2018), and Ali et al. (2018).The decarbonated samples were weighed and packed in tin capsules and introduced into an Elemental Analyzer (Flash EA 2000 HT) through an auto sampler. Through combustion, CO_2 gas was produced and introduced into a Continuous Flow Isotope Ratio Mass Spectrometer (MAT 253) coupled with Con-Flow IV interface for isotopic analysis. Repeat measurements were done at different intervals to check the reproducibility of the results (Ali et al., 2018).

Elemental analysis was conducted on 30 mg of powdered sediment from each sample. The digestion of each sample was carried out in a Teflon tube using a two-step process. In the first step, the sediment was allowed to digest using a 5ml mixture of hydrofluoric acid (HF) and nitric acid (HNO_3) followed by 1 ml of perchloric acid ($HClO_4$), covered with a Teflon cap, and heated to ~120°C using open digestion (Q-Block operating system). The heating continued until the acid fumes stopped evaporating from the tube and the sample became completely dry. The dried residue of the first step was processed for the second step by adding a 5ml mixture of $HF + HNO_3$ (1:2 ratio) followed by 1 ml of $HClO_4$; the sample was again capped and heated to ~150°C. The tubes were checked for complete digestion of sediments by adding 2 ml of 5% HNO_3 and observing the clarity of the solution. If any part was still left, the process was repeated until it was completely digested. After that, a 2% HNO_3 solution was used to rinse the tube, and the sample was transferred in a volumetric flask to make a final volume of 50 ml. A similar digestion procedure was followed for a standard reference material (U.S. Geological Survey SGR 1B) and blanks. The digested samples, standards, and blanks were analyzed using the Agilent Quadrupole 7700 ICP-MS instrument installed at the Birbal Sahni Institute of Palaeosciences, Lucknow for trace elemental concentrations of Rb and Sr. The error was <10%.

Loss on ignition (LOI) was employed to estimate the total organic content in the sediments. For this analysis, sequential heating of the powdered sediment samples was undertaken in a muffle furnace (Dean, 1974; Bengtson and Enell, 1986; Rawat et al., 2015; Dubey et al., 2018). In this process, ~5 g of finely powdered sample (after quartering and coning) was placed in a quartz crucible and kept in a preheated oven with a constant temperature of 110°C for 12 hours. Weighing of the oven-treated samples was done to estimate the percentage loss of moisture (Eq. 1). Two additional steps of heating were carried out in a muffle furnace. For the combustion of organic matter, the samples were kept in a pre-heated furnace (550°C) for 2 hours and then weighed. The last heat treatment at 950°C for 2 hours was used to estimate the carbonate fraction.

$$\text{LOI (weight \%)} = 100 \text{ x } [(n_2 - n_3)/(n_2 - n_1)] \quad (1)$$

Where, n_1 = weight of empty crucible; $n_2 = n_1$ + sample weight (before heating step), and $n_3 = n_1$ + sample weight (after heating step).

The grain size analysis was carried out on a laser particle size analyser (LS 13 320) from Beckman Coulter with a size range of 0.004–2000 µm. The samples were introduced after a pretreatment with H_2O_2 to remove the organic matter, 1N HCl to remove any carbonate fraction, and Na-hexametaphosphate to keep the grains dispersed.

RESULTS

Radiocarbon (accelerator mass spectrometry ^{14}C) ages and age-depth relationship

For establishing the chronology, four samples were dated using the accelerator mass spectrometry (AMS) radiocarbon technique at AMS radiocarbon dating laboratory, Direct-AMS, USA, and at the Physical Research Laboratory Ahmadabad, India (AMS^{14}C; Fig. 3, Table 1). The age-depth model was built on these four dates. The calculated ages were calibrated using intcal13 (Reimer et al., 2013). The age-depth relationship

https://doi.org/10.1017/qua.2020.22 Published online by Cambridge University Press

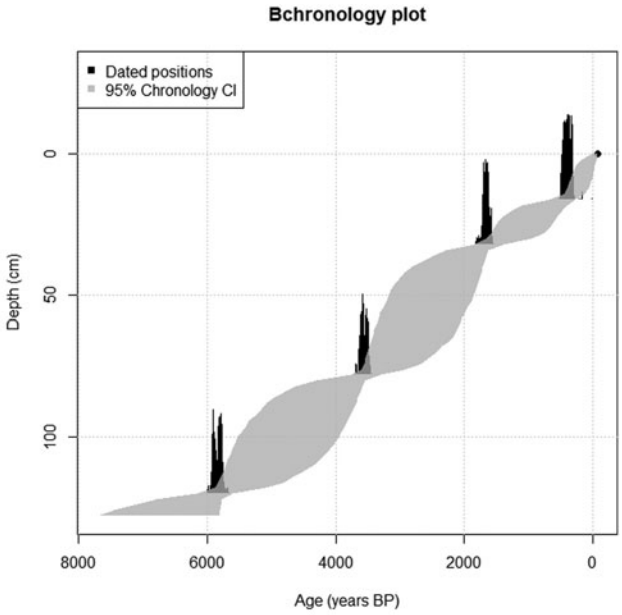

Figure 3. Bayesian age and depth chronology for the sediment core using R platform (version 3.5.0).

was modelled assuming the modern sample is of 2 ± 1 age; this is shown in Figure 3. From this age-depth model, the ages were interpolated for every sample of the core. The calibration and the age-depth model were done in R software using the Bchron package (R Core Team, 2019; Haslett and Parnell, 2008; Parnell, 2016).

Temporal changes in environmental proxies

The organic composition and grain size show significant variations in the sediment core (Fig. 4). The grain size shows an overall sandy-silty composition, where average sand, silt, and clay content are ~60%, 38%, and 2%, respectively. Although the clay percentage in the core is low, relatively higher values interpreted as a manifestation of aridity and hence important in understanding the paleoclimatic conditions (Ju et al., 2012). Total organic carbon (TOC) is low (~0.6%; ~6200 to 4500 cal yr BP) in the bottom of the core, a gradual increase is observed in the middle section (~4500 to 3400 cal yr BP), and an overall increasing trend is seen towards the top with some fluctuations at ~2700, 2250, and 1000 cal yr BP and at present. Similarly, organic carbon (Fig. 4) shows a gradually increasing trend and further complements the overall data set. The stable carbon isotope ($\delta^{13}C$) values in the Penzi-la sediment core vary from −19.9 to −25.6‰ with an average value of −22.4‰ and a range of 5.7‰ (Supplementary Table S1). The $\delta^{13}C$ values show a distinct temporal variability. The lower/bottom part of the sediment core (depth; 128–94 cm), which has an age range of ~6200–4500 cal. yrs. B.P., shows higher $\delta^{13}C$ values with an average of −20.4‰; maximum and minimum values are −19.9‰and −21.1‰, respectively. The subsequent section (between 92 and 74 cm; age ~4500–3400 cal yr BP) shows lower $\delta^{13}C$ values of the soil organic matter (SOM), with an average of −22.1‰, a maximum value of −20.1‰, and a minimum value −23.1‰. This is followed by a gradual lowering of $\delta^{13}C$ values (at depth; 72–34 cm) punctuated by three higher $\delta^{13}C$ excursions during ~3400–1500 cal yr BP (Fig. 4). This section with an average $\delta^{13}C$ value of −22.7‰ has yielded maximum and minimum values of −20.3‰ and −23.9‰, respectively. The top ~32 cm (~1500 cal yr BP to present) of the profile follow a similar trend with gradual lowering in the $\delta^{13}C$ values towards the top though with slightly higher values at ~400 cal yr BP. The top 6 cm of the core have yielded almost consistent values of around −25.5‰ (Fig. 4). These values are consistent with the modern isotope values of the SOM and surrounding vegetation (Supplementary Table S2). The Rb/Sr ratio of elemental concentrations also complements other proxies and has a clear trend. The older (lower; ~6200–4500 cal yr BP) part of the core is characterized by an increasing trend in the Rb/Sr ratio. Subsequently (~4500–3400 cal yr BP) a stable trend with a relatively lower Rb/Sr ratio is observed; this is followed by a gradual (fluctuating) but increasing ratio during the period around 3400–1500 cal yr BP. A stable ratio is observed between ~1500 and 300 cal yr BP and is followed by a gradual lowering.

Table 1. Ages obtained by accelerator mass spectrometry ^{14}C dating.

Sample no.	Sample ID	Depth (cm)	Dating material	AMS ^{14}C age (yr BP)	Error (1σ)
1	PNZ-8[a]	16	Bulk sediment	418	136
2	PNZ-31[a]	32	Bulk sediment	1647	92
3	PNZ-39[b]	78	Bulk sediment	3562	109
4	PNZ-60[b]	120	Bulk sediment	5821	171

[a]Direct-AMS, USA
[b]Physical Research Laboratory, Ahmedabad, India

Principal Component Analysis

Principal Component Analysis (PCA) was carried out to check the association of samples with the biotic characteristics (i.e., TOC, total organic content (OC), moisture, and $\delta^{13}C$ values) using the R platform (R Core Team 2019) vegan package from the CRAN project (Oksanen et al., 2019). Screeplots suggest that only one component among the four is sufficient to explain the variability among the samples (Fig. 5a). The biplot shows that, except for samples 5, 51, 55, and 56, all the samples have been spread across the PCA 1 axis that explains 54.4% of the variability among the data (Fig. 5b). Further, the TOC, OC, and moisture are on the negative axis of PCA 1 and $\delta^{13}C$ is on the positive axis of PCA 1. The OrgC lies on the negative side of the PCA 2 axis, and moisture is on the negative side of the PCA 3 axis. We note that the first two PCA axes could explain 74% of the variability among samples. However, as per the screeplot shown in Fig. 5c, the first PCA axis accounts for a significant amount

https://doi.org/10.1017/qua.2020.22 Published online by Cambridge University Press

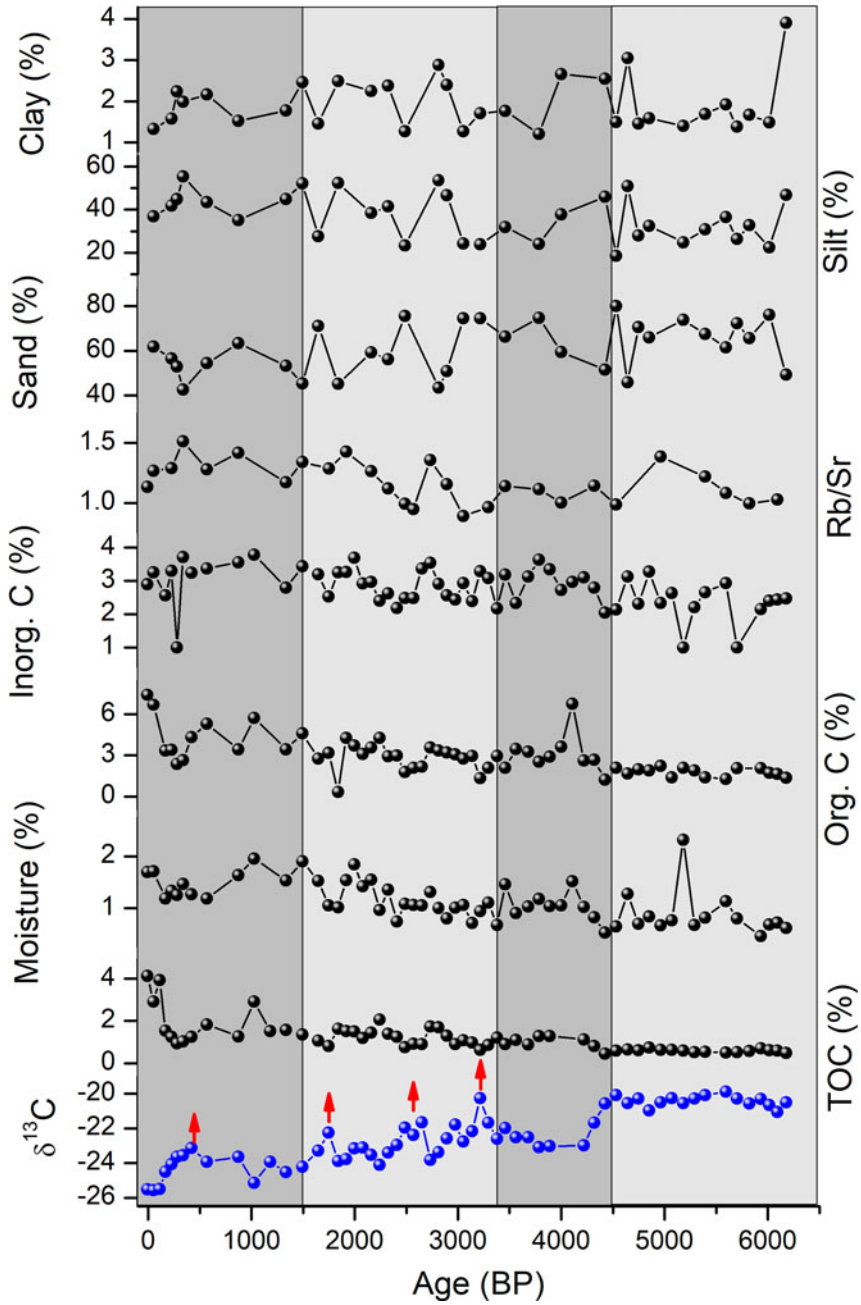

Figure 4. Temporal variability and correlation in measured $\delta^{13}C$ value (‰; VPDB), total organic carbon (TOC; %), moisture content (%), organic and inorganic carbon (%), Rb/Sr ratio and grain size parameters (sand, silt, and clay %). (For interpretation of the references to color in this figure legend, the reader is referred to the web version of this article.)

of variability (54.4%). Additionally, sample scores of the PCA 1 axis are well correlated to TOC (–0.94), OC (–0.90), and $\delta^{13}C$ (0.84). All three parameters (TOC, OC, and $\delta^{13}C$) are linked to vegetation, which therefore makes them important proxies for reconstructing the past vegetation and climate. Organic matter degradation may have significant influence on TOC and OC, but it has an insignificant effect on carbon isotopic composition (Hodell and Schelske, 1998; Meyers and Lallier-Vergés, 1999). For that reason, the carbon isotopic composition of organic matter in sediment thus preserves environmental signals from when the organic matter was formed (Yanhong et al., 2006) and hence has been used as the primary basis of interpretation in this study; it is complemented by other proxies like Rb/Sr, grain size, TOC, and LOI parameters.

Significance of $\delta^{13}C$ and Rb/Sr data

$\delta^{13}C_{org}$ records from terrestrial plant tissues and soil organic matter (SOM) derived from C_3-dominated vegetation has

https://doi.org/10.1017/qua.2020.22 Published online by Cambridge University Press

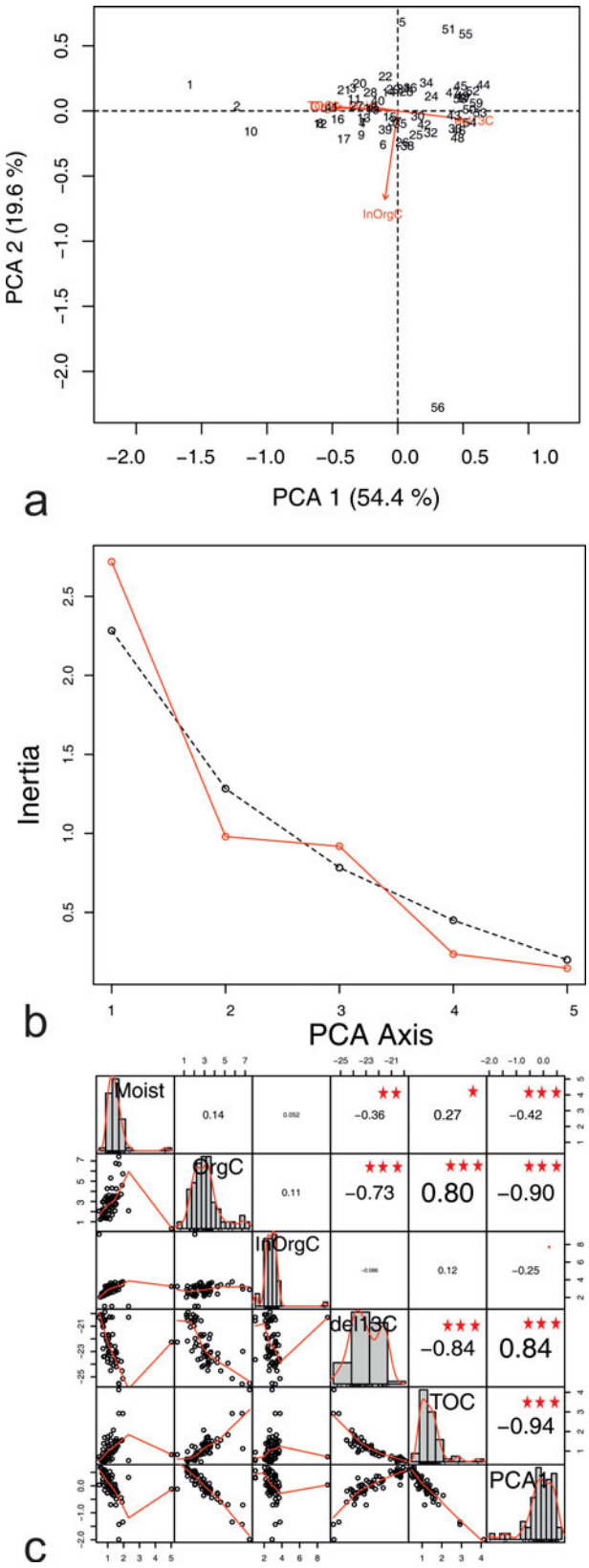

Figure 5. Principal component analysis (PCA) to check the variability among the samples. Screeplot (a) suggests only one component is sufficient to explain the significant variability among the samples. The biplot (b) suggests that total organic carbon and OC lie on PCA 1 (-ve) axis and $\delta^{13}C$ lies on the + ve axis, and these results are corroborated by the correlation plots (c).

been used to reconstruct past climatic and ecological conditions (e.g., Cerling 1984; Quade et al. 1989, 1995; Kohn 2010, 2016). The mean annual precipitation, latitude, and altitude are the most significant controlling factors of $\delta^{13}C$values of terrestrial C_3 plants (Diefendorf et al., 2010; Basu et al., 2015, 2019; Kohn 2016; Rao et al., 2017). Hence, the $\delta^{13}C$ value of SOM under C_3-dominated vegetation has a negative correlation with precipitation (Kohn, 2010; Rao et al., 2013, 2017; Basu et al., 2015, 2019) and has been successfully used to reconstruct climate variability in the eastern Himalaya (Ali et al., 2018). The $\delta^{13}C$-based investigations of modern plant and SOM samples in the Penzi-la show a C_3-dominated vegetation (alpine meadow; average $\delta^{13}C = -25.5‰$). These values suggest a precipitation of around 450 mm and are in agreement with the modern-day precipitation data (Supplementary Fig. S2; Sharma et al., 2018; Climate Research Unit (CRU)-TS 4.03 data). We are confident that the carbon isotopic composition of plants in the Penzi-la area will portray the variations in precipitation/hydrological conditions (Francey and Farquhar, 1982; Sternberg et al., 1984; Ali et al., 2018).

The temporal variation in the Rb/Sr ratio of loess–paleosol and lacustrine sequences has successfully been used as a proxy for the degree of pedogenesis and weathering (Dasch, 1969; Chen et al., 1999; Jin et. al., 2006; Chang et al., 2013). Sr is found in association with calcium-bearing minerals (Sr substitutes for calcium in the lattices of silicate/carbonate minerals) that are easy to break down during the weathering process (Jin et al., 2006; Chang et al., 2013). Rb substitutes for potassium, displays inert behaviour, and is resistant to weathering; hence, it is sequestered in the residual phases (Jin et al., 2006). The original Rb/Sr ratio is preserved in lacustrine sediments as they are deposited in a closed system (Jin et al., 2006). Therefore, in closed-lake sediments, during favourable climate conditions (high run-off), the Rb/Sr ratio will be high as both Rb and Sr will come into the system. However, during periods of lower run-off, the easily weathered Sr will be more available, and hence the ratio will be lower (Jin et al., 2006).

DISCUSSION

Evolution of the sedimentary sequence

The significance of the present study is in its location (transitional zone) and multiproxy approach wherein several proxies have been simultaneously used to address the hydroclimatic variability in one of the world's harshest climate regions (Ladakh—cold desert; see Fig. 1). The study site does not have any significant drainage systems, and the deposition of the locally available sediments relies upon snow melt and ISM-induced surface runoff and hence provides an opportunity to infer the local hydroclimatic conditions. Based on the variations in the multiproxy data (see Fig. 4), four prominent phases of climate variability have been identified in the Penzi-la sediment core, Zanskar Valley. The sediments of the core bottom (~6200–4500 cal yr BP) are dominated by sand

https://doi.org/10.1017/qua.2020.22 Published online by Cambridge University Press

(66%) and followed by silt (32%) with only a minor contribution from clay. The proportions of sand and silt throughout the profile are almost similar, suggesting a more or less analogous depositional environment. The moisture content and the organic carbon are low in this part. The higher $\delta^{13}C$ values (avg. −20.4‰) in this zone suggest low water availability. Low TOC is also attributed to drier climatic conditions restricting the vegetation growth (Ali et al., 2018; Srivastava et al., 2018). These observations are further complemented by the relatively lower Rb/Sr ratio in this zone. The results suggest an overall lower availability of water during ~6200–4500 cal yr BP. Subsequently, a significant increase in TOC, organic carbon content, and moisture percentages is observed, implying improvement in climate conditions during ~4500–3400 cal yr BP (see Fig. 4). This phase is characterized by a prominent lowering of $\delta^{13}C$ values (avg. −22.1‰), which further points towards the increased availability of moisture. The Rb/Sr ratio shows moderate values in this zone suggesting relatively higher runoff. During the interval between ~3400 and 1500 cal yr BP, a progressive lowering of $\delta^{13}C$ values is observed, suggesting climate amelioration. This ameliorating trend is punctuated by three prominent dry phases (less negative $\delta^{13}C$ values) at ~3200, 2500, and 1750 cal yr BP (see Fig.4). This zone is further characterized by an increasing trend in TOC, moisture content, and Rb/Sr ratio. The corresponding grain size also shows a response to these climatic changes, and the clay content is relatively higher for the phase with the less negative $\delta^{13}C$ values. During the last ~1500 cal yr BP, a gradual improvement in climatic conditions is seen with a dry spell at ~400 cal yr BP. Higher sand content, TOC, moisture, and organic carbon (%) and low $\delta^{13}C$ values towards the top (after ~400 cal yr BP) are attributed to enhanced hydroclimatic conditions. The very low content of sand at ~400 cal yr BP further suggests low-energy runoff conditions.

Climatic implications and comparison with other sites

The present study documents a quasi-continuous mid–late Holocene record of hydroclimatic variability from the Zanskar Valley, situated in a transitional climate zone towards the orographic limit of ISM precipitation in the NW Himalaya. Detailed paleoclimatic reconstructions from the NW Himalaya are scanty and restricted to the eastern sector of Ladakh (Tso Kar [Wünnemann et al., 2010]; Tso Moriri [Leipe, Demske, and Tarasov, 2014; Leipe, Demske, Tarasov, Wünnemann, et al., 2014; Mishra et al., 2015]). The eastern sector is characterized by extreme climatic conditions with an annual precipitation of less than 90 mm (Wünnemann et al., 2010), and the effect of ISM is minimal (Mishra et al., 2015). Contrary to this, our study area is located in the transitional zone of ISM influence and receives a moderate amount of precipitation (~450–600 mm) and hence is a better location for understanding the hydroclimatic variability. The present study shows fluctuating hydroclimatic conditions during last ~6200 cal yr BP and shows a good correlation with speleothem and paleo-lake records with other local (Higher Himalayan) and regional sites. Therefore, it is desirable to see whether the hydroclimatic conditions reconstructed using carbon isotope ratios of SOM from the Penzi-la are synchronous with other climatic records. We compared our $\delta^{13}C$-based climatic record with regional paleoclimatic reconstructions based on different proxies in order to delineate the forcing factors behind these events; these comparisons are outlined below (see Fig. 4).

Mid-Late Northgrippian (~6200–4500 cal yr BP)

On the basis of $\delta^{13}C$ values, Rb/Sr ratio, low TOC, LOI, and sand (%), our study indicates a stable but relatively dry climate during the mid-late Northgrippian (~6200–4500 cal yr BP). This dry phase is in accordance with the youngest Southern Zanskar Glacial Stage (SZS-1; Sharma and Shukla, 2018; Sharma et al., 2018) that occurred after 6.3 ka and before 5.1 ka in the Zanskar Valley and has been attributed to an overall weakened ISM (Wünnemann et al., 2010; Bhushan et al., 2018; Sharma and Shukla, 2018). The SZS-1 glacial advance has been attributed to millennial-scale cooling events (Sharma and Shukla, 2018). Based on the changes in the pollen spectra, reduced local pollen production, and increasing scores of desert and decreasing scores of tundra revealed in the biome reconstruction, a reduction in moisture availability after ~6200 cal yr BP is indicated from the Tso Moriri lake (Leipe, Demske, Tarasov, 2014; Leipe, Demske, Tarasov, Wünnemann, et al., 2014). Similarly, Wünnemann and colleagues (2010) observed that this period is marked by a decline in detrital input due to reduced melt water flux and that the Tso Kar (lake) shrank gradually after 7000 cal yr BP and attained its lowest stand at about 4200 cal yr BP. High-resolution paleoclimatic studies from the adjacent regions also show a similar trend of declining moisture availability during this time (Ranhotra et al., 2001; Kotlia and Joshi, 2013; Kotlia et al., 2015; Bali et al., 2017; Bhushan et al., 2018; Srivastava et al., 2018).

A multiproxy climatic reconstruction from the central Himalaya has also reported high-frequency climatic variability with an overall dryness during ~5400 to ~3800 cal yr BP (Srivastava et al., 2018). A cold, dry climate during a weak phase of the ISM is also well recorded between ~5 and 4 ka from the Dongge Cave, China (Wang et al., 2005) and also in the Guliya ice core record (Thompson et al., 1997). This weakening of ISM is also reported from the core monsoon zone of India, specifically from Lonar Lake (Sarkar et al., 2015) and Noni Tal, Madhya Pradesh (Kumar et al., 2019). $\delta^{13}C_{wax}$ data of Sarkar and colleagues (2015) and phytolith index values along with higher $\delta^{13}C$ (Prasad, V. et al., 2014) further indicate drier climatic conditions during this period.

The decreasing trend in the rainfall pattern post ~6000 cal yr BP is attributed to the progressive decrease in insolation and a southward shift of the ITCZ after the mid Holocene (Fig. 6; Fleitmann et al., 2007; Sarkar et al., 2015; Ali

https://doi.org/10.1017/qua.2020.22 Published online by Cambridge University Press

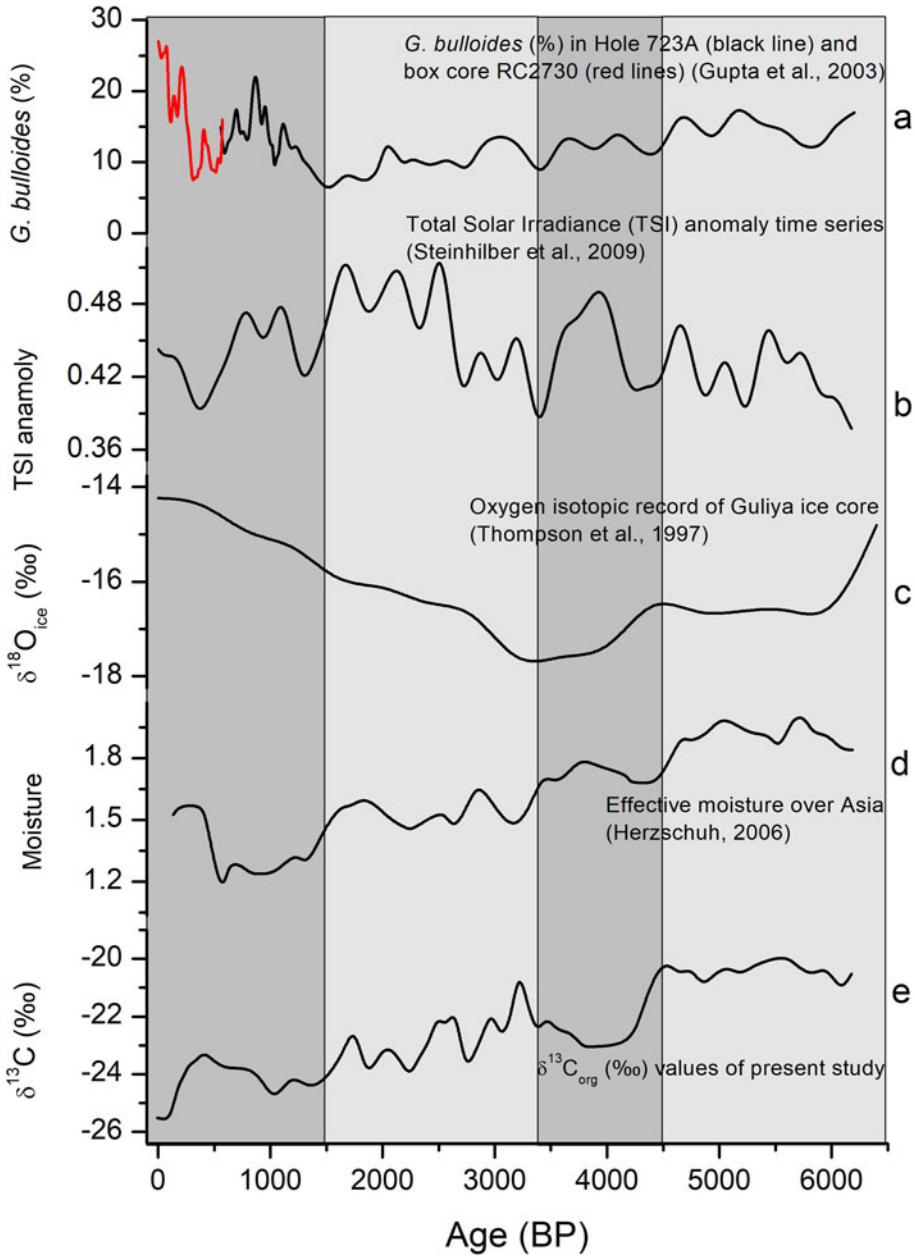

Figure 6. Indian Summer Monsoon/ hydroclimatic variability through regional comparison of different data sets and the Penzi-la data. The light grey bands represent moisture deficiency, while the darker bands show better hydroclimatic conditions.

et al., 2018). The continuous retreat of the ITCZ towards the south and its effect on the ISM intensity (weakening) has been attributed to a gradual response to decreasing orbitally induced solar insolation from both terrestrial and marine archives (Wang et al., 2001; Gupta et al., 2003; Fleitmann et al., 2007; Dutt et al., 2015; Dixit et al., 2014, 2018). Furthermore, the increased ice rafting and corresponding reduction in sea surface salinity resulted in a distinctly cooler phase between 6.5 and 3.7 ka yr BP (Moros et al., 2004; Wiersma and Renssen, 2006). Comparison and correlation between the present data and the above-discussed studies from different ecological systems and diverse geographical settings are in agreement and support a global cooling phase (dry) during the mid-Late Northgrippian.

Late Northgrippian to Early Meghalayan (~4500–3400 cal yr BP)

Following a cool and dry mid-Holocene (Mid-Late Northgrippian), an amelioration in climatic conditions is observed between ~4500 and 3400 cal yr BP. Lower $\delta^{13}C$ values and stable Rb/Sr ratios along with relatively higher TOC and organic carbon content in the Penzi-la sediment core are observed, and more positive hydroclimatic conditions are indicated. Our results are in accordance with the inferences drawn from detrital geochemical proxies of weathering and erosion from monsoon-dominated central Himalaya (Bhushan et al., 2018), suggesting a weak to moderate ISM during ~3500–2040 cal yr BP. Similarly, on the basis of

https://doi.org/10.1017/qua.2020.22 Published online by Cambridge University Press

low $\delta^{13}C$ values recorded at ~4000 cal yr BP and from ~3500 to 3170 cal yr BP, Rawat and colleagues (2015) suggested centennial-scale high precipitation conditions in the Chandra Valley. In monsoon-dominated Kedarnath Valley, an enhanced insolation-driven ISM has been reported (Srivastava et al., 2018). The improved hydroclimatic conditions are in accordance with an increase in total solar irradiance (Steinhilber et al., 2009) and *Globigerina bulloides* percentage (Gupta et al., 2003), as well as a slight increase in mean effective moisture over central Asia (Fig. 6; Herzschuh, 2006). We propose that enhanced solar irradiance may have resulted in enhanced snow and glacial melt as well as strengthening of the ISM, thereby creating favourable conditions for vegetation growth as evidenced by lowering of $\delta^{13}C$ values and enhancement in TOC content.

Middle Meghalayan (~3400–1500 cal yr BP)

During this phase an overall improvement in the hydrological conditions is observed; however, this trend is interrupted by three centennial-scale dry events. These dry events exhibited progressively lower amplitudes at ~3200, 2500, and 1750 cal yr BP respectively (see Fig. 4).The incidence of such abrupt drying events during the Middle Meghalayan (late Holocene), in addition to the 4.2 ka and LIA events, also deserves careful attention, but has rarely been explored (Park et al., 2019 and references therein). The ~3200 and ~2400 cal yr BP dry/cooling events are reported from other Northern Hemisphere climate records and are suggested to have arisen from a solar-induced shift in atmospheric circulation (Svendsen and Mangerud, 1997; Martin-Puertas et al., 2012; Kaniewski and Van Campo, 2017; Harning et al., 2018; Park et al., 2019).The third cooling event, at ~1700 cal yr BP, is broadly comparable with the Dark Ages cooling period also termed the Late Antique LIA (Ljungqvist, 2010; Büntgen et al., 2016). A volcanic eruption–driven abrupt summer cooling that was probably sustained by positive feedback loops of ocean-heat content and sea-ice extension has been implicated for this event (Miller et al., 2012; McGregor et al., 2015; Büntgen et al., 2016). In the case of the Himalayan glacier advances, this phase corresponds to the MOHITS1C glacial advance (regional age ~1500 ± 200 yr) that has been reported from the southern and eastern portions of the Himalaya and suggested to have been driven by Northern Hemisphere climatic events (Murari et al., 2014). However, the exact reasons for this dry event that does not bear any significant correlations with either the ice core or speleothem data is unclear and needs further investigation.

Apart from these cool/dry events, an overall gradual ameliorating trend in the hydroclimatic conditions is observed during this period (~3400–1500 cal yr BP) and correlates well with a progressive increase in total solar irradiance and the $\delta^{18}O$ values of Guliya ice core. Correlations with the $\delta^{18}O$ record of the Guliya ice core have been used as a proxy for monsoon strength. A comparable moist climate during ~3500–1800 cal yr BP using geochemical proxies from Badanital (central Himalaya; Kotlia and Joshi, 2013) and a warm and less humid climate during ~3200–2200 cal yr BP from Triloknath using palynological data (western Himalaya [Bali et al., 2017]) have been reported. High-resolution speleothem data from Sainji Cave (central Himalaya [Kotlia et al., 2015]) also recorded an amelioration in climate during ~3000–2000 cal yr BP. In Chandra Valley, the period between ~3340 and 2030 cal yr BP records growth of a diverse vegetation cover with continuous expansion of wetland taxa resulting ultimately in the development of a mixed coniferous and broad-leaved forest (Rawat et al., 2015). Further, the study has also reported similar lowering of $\delta^{13}C$ values and an increase in LOI percentage from ~2900 to 2030 cal yr BP, which indicates dominance of C_3 vegetation under a warm and wet climatic condition. The increased moisture availability has been attributed to both snow and glacial melt, as well as from ISM moisture. Although the climatic inferences from the Tso Moriri lake (Leipe, Demske, Tarasov, 2014; Mishra et al., 2015) are not in agreement with these data sets, the climate records from most of the ISM-influenced regions indicate the strengthening of ISM during this phase (Yadava and Ramesh, 2001; Chauhan et al., 2010; Prasad, S. et al., 2014; Rawat et al., 2015). The disagreement between the previous studies (Tso Kar and Tso Moriri lakes) and our results may be attributed to the contribution of ISM and/or the attenuating impact of the westerlies (Wünnemann et al., 2010; Leipe, Demske, Tarasov, 2014; Leipe, Demske, Tarasov, Wünnemann, et al., 2014; Mishra et al., 2015) to these records. Our interpretations receive enhanced confidence from the suggestions that high monsoonal runoff has been recorded from the Indus River during the period from ~3500 to 2200 cal yr BP, based on varve thickness/counts verified by conventional and AMS ^{14}C dating (von Rad et al., 1999). This phase of monsoon revival and warmer conditions in strengthening ISM conditions corresponds to the increased sea surface temperature in the northeastern Arabian Sea from ~3300 to 1500 yr BP (Doose-Rolinski et al., 2001).

Late Meghalayan (~1500 cal yr BP to present)

Progressive increase in the moisture availability during this phase is punctuated by a prominent dry spell at ~400 cal yr BP (LIA). The observed climatic amelioration during the ~1500–400 cal yr BP coincides with the moderate expansion of broad-leaved, non-arboreal pollen and ferns recorded between ~1160 and 650 cal yr BP from the Chandra Valley (western Himalaya) under a climate amelioration (Rawat et al., 2015). This ameliorating trend is analogous to a strengthening ISM and has been reported from other Himalayan basins using different proxies (Bhattacharyya and Chauhan, 1997; Chauhan and Sharma, 2000; Kar et al., 2002; Kotlia and Joshi, 2013; Sanwal et al., 2013; Sinha et al., 2015; Bali et al, 2017; Bird et al., 2017; Srivastava et al., 2018). A prominent increase in the $\delta^{13}C$ values with lower TOC and LOI parameters suggests a dry climate at ~400cal yr BP (LIA cooling event). Relatively higher clay and silt content (low sand) during this time may be attributed to long-

https://doi.org/10.1017/qua.2020.22 Published online by Cambridge University Press

distance wind transport implying an arid cold climate (Ju et al., 2012). A similar phase (~650–350 cal yr BP) has recorded a decline in most broad-leaved taxa and meadow vegetation in the Chandra Valley and has been attributed to a LIA cold-dry climate (Rawat et al., 2015). The LIA climate response has been recorded from different proxies ranging from glacier advance (Owen et al., 1996) to lake records from different sectors of Himalaya with some chronological mismatch (Bhattacharyya, 1988; Mazari et al., 1996; Bhattacharyya and Chauhan, 1997; Chauhan et al., 2000; Sharma and Chauhan, 2001; Kar et al., 2002; Chauhan, 2006; Rawat et al., 2015; Bali et al., 2017; Srivastava et al., 2018). Despite the chronological disparity, the LIA cooling seems to have been present across the region. Although the Northern Hemisphere LIA glacial advances took place during 1400–1900 AD, the Himalayan LIA glacial advance occurred between 1300 and 1600 AD, slightly earlier than the coldest period in the Northern Hemisphere (Rowan, 2017). This earlier cooling in the Himalaya has been attributed to a southward shift in the Asian monsoon, increased westerly winter precipitation, and wetter conditions (Rowan, 2017).

Subsequently, after the LIA cooling, there is a decrease in $\delta^{13}C$ and Rb/Sr values and an increase in TOC and LOI parameters, suggesting a wetter hydroclimate. A decrease in clay and an increase in the sand content imply that the climate was getting wetter under increasing moisture availability. Kumar and colleagues (1994) derived winter warming trends in an all-India temperature series and 0.08°C/10 yr for the NW region for 1901–1987. A similar and significant increasing trend in the winter temperature has been reported from the western Himalaya that exceeds the global averages (Bhutiyani et al. 2010).It is also reported that Uttarakhand is experiencing a significant warming and the temperature in hilly areas is rising more prominently than on the plains (Mishra 2017). Similarly, Shrestha and colleagues (1999) found increases in winter maxima of for all Nepal, Himalayan, and Trans-Himalayan stations. Cook and colleagues (2003) found indications of warming since 1960 at Kathmandu only in the period from October to January. Regional (high Asia) climate proxy records also show twentieth-century warming in the context of the last millennium (D'Arrigo et al., 2001; Zhu et al., 2008; Yadav et al., 2011; Shekhar et al., 2017). This implies that an increase in temperature enhanced the snow and glacial melt and the moisture holding capacity of the atmosphere that directly affect the precipitation patterns and intensity (Trenberth et al., 2003).

Our results suggest a gradual enhancement of hydroclimatic conditions in the Zanskar Valley since ~6200 cal yr BP and is in accordance with other studies (Chauhan et al., 2000; Kale et al., 2000, 2003; Phadtare, 2000; Thomas et al., 2007; Sanwal et al., 2013; Bhattacharya et al., 2014; Kotlia et al., 2015; Bali et al., 2017). However, this trend is punctuated by abrupt reversals/dry periodsin the Zanskar Valley. Similar local events have been reported from the Dewar Tal (central Himalaya) where a cool and dry climate has been inferred at ~2500–2300, 2000–1400, and 400 cal yr BP (Chauhan and Sharma, 2000) that broadly corresponds to a cold, dry climate in the Kunzum pass area at around 2300–1500 cal yr BP (Chauhan et al., 2000).The mid-late Holocene has been a time of enhanced insolation (Crowley and North, 1991; Rupper et al., 2009) and a relatively stronger ISM. We attribute the gradual enhancement of hydrological conditions to total solar irradiance. The last ~1000 years are very important in the Holocene because two major climate events, including the MCA, which created wet conditions between 1050 and 600cal yr BP, and the LIA, a cold/dry period from 450 to 150BP,occurred during this time (Lamb, 1965; Crowley, 2000; Mann et al., 2009; Polanski et al., 2014; Dixit and Tandon, 2016). Both regional and global proxy reconstructions show spatial and temporal heterogeneity in these two climate events which have been ascribed to a complex array of forcings, feedbacks, and internal variability operating in the climate system (Agnihotri et al., 2002; Kaufman et al. 2009; Yadav et al., 2011; Fernández-Donado et al. 2013; Lehner et al. 2013; Polanski et al., 2014; Dixit and Tandon, 2016). However, solar output variations have been suggested as the main driver of both ISM (Neff et al., 2001; Gupta et al., 2003) and the North Atlantic cycles (Bond et al., 2001) and as the primary climate modulator.

CONCLUSIONS

Our multiproxy paleoclimatic record from the Penzi-la pass shows four climatic phases with an overall gradual improvement in the hydroclimatic conditions since ~6200 cal yr BP. Abrupt dry spells occurred at ~3300, 2600, 1700, and 400 cal yr BP and deserve careful attention in future investigations. Contrary to the earlier studies in the NW Himalaya, our results show increasingly positive hydroclimatic conditions in this transition zone between the Higher Himalaya and Trans-Himalaya (Zanskar Valley).Notable swings of climate like the MCA and LIA and their local and regional correlations indicate a common insolation forcing. This study indicates that the abrupt changes in the hydroclimate of the Zanskar Valley were also coupled with the northern latitude climatic events, although changes in solar radiation have been the primary driver.

ACKNOWLEDGMENTS

The authors are thankful to the Director, Birbal Sahni Institute of Palaeosciences, Lucknow, India, for his support and for providing infrastructural facilities (the Sophisticated Analytical Instruments Facilities at the Birbal Sahni Institute of Palaeosciences, publication no. 45/2019-20). Special thanks go to the Governments of Jammu and Kashmir for their help and for providing necessary permissions during the fieldwork. Thanks are also due to the field staff (Mr. Shenge Takpa) who worked tirelessly in the harsh conditions during fieldwork. Authors are grateful to the editor and anonymous reviewers for their valuable suggestions and constructive comments, which helped us improve the manuscript.

SUPPLEMENTARY MATERIAL

The supplementary material for this article can be found at https://doi.org/10.1017/qua.2020.22.

https://doi.org/10.1017/qua.2020.22 Published online by Cambridge University Press

REFERENCES

Agnihotri, R., Dutta, K., Bhushan, R., Somayajulu, B., 2002. Evidence for solar forcing on the Indian monsoon during the last millennium. *Earth and Planetary Science Letters* 198, 521–527.

Agrawal, S., Sanyal, P., Sarkar, A., Jaiswal, M.K., Dutta, K., 2012. Variability of Indian monsoonal rainfall over the past 100 ka and its implications to C_3–C_4 vegetational Change. *Quaternary Research* 77, 159–170.

Ali, S.N., Dubey, J., Ghosh, R., Quamar, M.F., Sharma, A., Morthekai, P., Dimri, A.P., Shekhar, M., Arif, M., Agrawal, S., 2018. High frequency abrupt shifts in the Indian summer monsoon since Younger Dryas in the Himalaya. *Scientific Reports* 8, 9287.

Ali, S.N., Juyal, N., 2013. Chronology of late quaternary glaciations in Indian Himalaya: a critical review. *Journal of the Geological Society of India* 82, 628–638.

Bali, R., Chauhan, M.S., Mishra, A.K., Ali, S.N., Tomar, A., Khan, I., Singh, D.S., Srivastava, P., 2017. Vegetation and climate change in the temperate-subalpine belt of Himachal Pradesh since 6300 cal. yrs. B.P., inferred from pollen evidence of Triloknath palaeolake. *Quaternary International* 444, 11–23.

Banerji, U.S., Arulbalaji, P., Padmalal, D., 2020. Holocene climate variability and Indian Summer Monsoon: An overview. *The Holocene*, 1–30. doi.org/10.1177/0959683619895577.

Basu, S., Agrawal, S., Sanyal, P., Mahato, P., Kumar, S., Sarkar, A., 2015. Carbon isotopic ratios of modern C3–C4 plants from the Gangetic plain, India and its implications to paleovegetational reconstruction. *Palaeogeography, Palaeoclimatology, Palaeoecology* 440, 22–32.

Basu, S., Sanyal, P., Pillai, A.A.S., Ambili, A., 2019. Response of grassland ecosystem to monsoonal precipitation variability during the Mid-Late Holocene: Inferences based on molecular isotopic records from Banni grassland, western India. *PloS one* 14, e0212743.

Bengtsson, L., Enell, M., 1986. Chemical analysis. In B.E. Berglund (Ed): *Handbook of Holocene Palaeoecology and Palaeohydrology*. Wiley, Chichester, 423–445.

Beniston, M., 2006. Mountain weather and climate: a general overview and a focus on climatic change in the Alps. *Hydrobiologia,* 562, 3–16.

Benn, D.I., Owen, L.A., 1998. The role of the Indian summer monsoon and the mid–latitude westerlies in Himalayan glaciations: review and speculative discussion. *Journal of the Geological Society of London,* 155, 353–363.

Bhattacharya, F., Rastogi, B.K., Thakkar, M.G., Patel, R.C., Juyal, N., 2014. Fluvial landforms and their implication towards understanding the past climate and seismicity in the northern Katrol Hill Range, western India. *Quaternary International* 333, 49–61.

Bhattacharyya, A., 1988. Vegetation and climate during postglacial in the vicinity of Rohtang Pass, Great Himalayan Range. *Pollen et Spores* 30, 417–427.

Bhattacharyya, A., Chauhan, M.S., 1997. Vegetational and climatic changes during recent past around Tipra Bank Glacier, Garhwal Himalaya. *Current Science* 72, 408–412.

Bhushan, R., Sati, S.P., Rana, N., Shukla, A.D., Mazumdar, A.S., Juyal, N., 2018. High-resolution millennial and centennial scale Holocene monsoon variability in the Higher Central Himalayas. *Palaeogeography Palaeoclimatology, Palaeoecology* 489, 95–104.

Bhutiyani, M.R., Kale, V.S., Pawar, N.J. 2010. Climate change and the precipitation variations in the northwestern Himalaya: 1866–2006. *International Journal of Climatology* 30, 535–548.

Bird, B.W., Lei, Y., Perello, M., Polissar, P.J., Yao, T., Finney, B., Bain, D., Pompeani, D., Thompson, L.G., 2017. Late-Holocene Indian summer monsoon variability revealed from a 3300-year-long lake sediment record from Nir'pa Co, southeastern Tibet. *The Holocene* 27, 541–552.

Birks, H.H., Birks, H.J.B., 2006. Multi-proxy studies in palaeolimnology. *Vegetation History and Archaeobotany* 15, 235–51.

Bond, G., Kromer, B., Beer, J., Muscheler, R., Evans, M.N., Showers, W., Hoffmann, S., Lotti-Bond, R., Hajdas, I., Bonani, G., 2001. Persistent solar influence on North Atlantic climate during the Holocene. *Science* 294, 2130–2136.

Bothe, O., Fraedrich, K., Zhu, X.H., 2011. Large-scale circulations and Tibetan Plateau summer drought and wetness in a high-resolution climate model. *International Journal of Climatology* 31, 832–846.

Büntgen, U., Myglan, V.S., Ljungqvist, F.C., McCormick, M., Di Cosmo, N., Sigl, M., Jungclaus, J., *et al*., 2016. Cooling and societal change during the Late Antique Little Ice Age from 536 to around 660 AD. *Nature Geoscience* 9, 231.

Cerling, T.E., 1984. The stable isotopic composition of modern soil carbonate and its relationship to climate. *Earth and Planetary Science Letters* 71, 229–240.

Cerling, T.E., 1992. Use of carbon isotopes in paleosols as an indicator of the P (CO2) of the paleoatmosphere. *Global Biogeochemical Cycles* 6, 307–314.

Chang, H., An, Z., Wu, F., Jin, Z.D., Liu, W., Song, Y., 2013. A Rb/Sr record of the weathering response to environmental changes in westerly winds across the Tarim Basin in the late Miocene to the early Pleistocene. *Palaeogeography, Palaeoclimatology, Palaeoecology* 386, 364–373.

Chauhan, M.S., 2006. Late Holocene vegetation and climate change in the alpine belt of Himachal Pradesh. *Current Science* 91, 1572–1578.

Chauhan, M.S., Mazari, R.K., Rajagopalan, G., 2000. Vegetation and climate in upper Spiti region, Himachal Pradesh during late Holocene. *Current Science* 79, 373–377.

Chauhan, M.S., Sharma, C., 2000. Late-Holocene vegetation and climate in Dewar Tal area, Inner Lesser Garhwal Himalaya. *Palaeobotanist* 49, 509–514.

Chauhan, O.S., Dayal, A.M., Basavaiah, N., Kader, U.S.A., 2010. Indian summer monsoon and winter hydrographic variations over past millennia resolved by clay sedimentation. *Geochemistry, Geophysics, Geosystems* 11, Q09009. doi:10.1029/2010GC003067.

Chen, J., An, Z., Head, J., 1999. Variation of Rb/Sr ratios in the loess-paleosol sequences of Central China during the last 130,000 years and their implications for monsoon paleoclimatology. *Quaternary Research* 51, 215–219.

Chen, J., Wang, H., Lu, H., 1996. Behaviours of REE and other trace elements during pedological weathering—evidence from chemical leaching of loess and paleosol from the Luochuan section in central China. *Acta Geologica Sinica* 9, 290–302.

Cook, E.R., Krusic, P.J., Jones, P.D., 2003. Dendroclimatic signals in long tree-ring chronologies from the Himalayas of Nepal. *International Journal of Climatology* 23, 707–732.

Crowley, T.J., 2000. Causes of climate change over the past 1000 years. *Science* 289, 270–77.

Crowley, T.J., North, G.R., 1991. *Paleoclimatology*. Oxford University Press, New York.

D'Arrigo, R., Jacoby, G., Frank, D., Pederson, N., Cook, E., Buckley, B., Nachin, B., Mijiddorj, R., Dugarjav, C., 2001. 1738 years of Mongolian temperature variability inferred from a tree ring

https://doi.org/10.1017/qua.2020.22 Published online by Cambridge University Press

width chronology of Siberian pine. *Geophysical Research Letters* 28, 543–546.

Dasch, E.J., 1969. Strontium isotopes in weathering profiles, deep-sea sediments, and sedimentary rocks. *Geochimica et Cosmochimica Acta* 33, 1521–1552.

Dean, W.E. Jr., 1974. Determination of carbonate and organic matter in calcareous sediments and sedimentary rocks by loss on ignition: Comparison with other methods. *Journal of Sedimentary Research* 44, 242–248.

Dearing, J.A., 2006. Climate-human-environment interactions: resolving our past. *Climate of the Past* 2, 187–203.

Dearing, J.A., Battarbee, R.W., Dikau, C.R., Larocque, I., Oldfield, F. 2006. Human–environment interactions: towards synthesis and simulation. *Regional Environmental Change* 6, 115–123.

Diefendorf, A.F., Mueller, K.E., Wing, S.L., Koch, P.L., Freeman, K.H., 2010. Global patterns in leaf 13C discrimination and implications for studies of past and future climate. *Proceedings of the National Academy of Sciences* 107, 5738–5743.

Dixit, Y., Hodell, D.A., Giesche, A., Tandon, S.K., Gázquez, F., Saini, H.S., Skinner, L.C., *et al*., 2018. Intensified summer monsoon and the urbanization of Indus Civilization in northwest India. *Scientific Reports* 8, 4225, doi:10.1038/s41598-018-22504-5.

Dixit, Y., Hodell, D. A., Petrie, C.A. 2014. Abrupt weakening of the summer monsoon in northwest India ~4100 yr ago. *Geology* 42, 339–342.

Dixit, Y., Tandon, S.K., 2016. Hydroclimatic variability on the Indian subcontinent in the past millennium: review and assessment. *Earth-Science Reviews* 161, 1–15.

Doose-Rolinski, H., Rogalla, U., Scheeder, G., Lückge, A., von Rad, U., 2001. High-resolution temperature and evaporation changes during the late Holocene in the northeastern Arabian Sea. *Paleoceanography and Paleoclimatology* 16, 358–367.

Dubey, J., Ghosh, R., Agrawal, S., Quamar, M.F., Morthekai, P., Sharma, R.K., Sharma, A., Pandey, P., Srivastava, V., Ali, S.N., 2018. Characteristics of modern biotic data and their relationship to vegetation of the Alpine zone of Chopta valley, North Sikkim, India: Implications for palaeovegetation reconstruction. *The Holocene* 28, 363–376.

Dutt, S., Gupta, A.K., Clemens, S.C., Cheng, H., Singh, R.K., Kathayat, G., Edwards, R.L., 2015. Abrupt changes in Indian summer monsoon strength during 33,800 to 5500 years BP. *Geophysical Research Letters* 42, 5526–5532.

Dutt, S., Gupta, A.K., Wünnemann, B., Yan, D., 2018. A long arid interlude in the Indian summer monsoon during ~4,350 to 3,450 cal. yr BP contemporaneous to displacement of the Indus valley civilization. *Quaternary International* 482, 83–92.

Ekart, D.D., Cerling, T.E., Montañez, I.P., Tabor, N.J., 1999. A 400 million year carbon isotope record of pedogenic carbonate: implications for paleoatmospheric carbon dioxide. *American Journal of Science* 299, 805–827.

Fernández-Donado, L., González Rouco, J.F., Raible, C., Ammann, C.M., Barriopedro, D., Garcia-Bustamante, E., Jungclaus, J.H., *et al*., 2013. Large-scale temperature response to external forcing in simulations and reconstructions of the last millennium. *Climate of the Past* 9, 393–421.

Finkel, R.C., Owen, L.A., Barnard, P.L., Caffee, M.W., 2003. Beryllium-10 dating of Mount Everest moraines indicates a strong monsoon influence and glacial synchroneity throughout the Himalaya. *Geology* 31, 561–564.

Fleitmann, D., Burns, S.J., Mangini, A., Mudelsee, M., Kramers, J.D., Villa, I.M., Neff, U., *et al*., 2007. Holocene ITCZ and Indian monsoon dynamics recorded in stalagmites from Oman and Yemen (Socotra). *Quaternary Science Reviews* 26, 170–188.

Francey, R.J., Farquhar, G.D., 1982. An explanation of $^{13}C/^{12}C$ variations in tree rings. *Nature* 297, 28–31.

Fuchs, G.R., 1982. Explanations of the geologictectonic map of the Himalaya. *Geological Survey of Austria*, Wien, 1–50.

Ganju, A., Nagar, Y.C., Sharma, L.N., Sharma, S., Juyal, N., 2018. Luminescence chronology and climatic implication of the late quaternary glaciation in the Nubra valley, Karakoram Himalaya, India. *Palaeogeography Palaeoclimatology, Palaeoecology* 502, 52–62.

Ghosh, R., Bera, S., Sarkar, A., Paruya, D.K., Yao, Y.-F., Li, C.-S., 2015. A ~50 ka record of monsoonal variability in the Darjeeling foothill region, eastern Himalayas. *Quaternary Science Reviews* 114, 100–115.

Giosan L., Clift, P.D., Macklin, M.G., Fuller, D.Q., Constantinescu, S., Durcan, J.A., Stevens, T., *et al*., 2012. Fluvial landscapes of the Harappan civilization. *Proceedings of the National Academy of Sciences of the United States of America* 109, 1688–1694.

Gupta, A.K., Anderson, D.M., Overpeck, J.T., 2003. Abrupt changes in the Asian southwest monsoon during the Holocene and their links to the North Atlantic Ocean. *Nature* 421, 354–357.

Harning, D.J., Geirsdóttir, Á., Miller, G. H., 2018. Punctuated Holocene climate of Vestfirðir, Iceland, linked to internal/external variables and oceanographic conditions. *Quaternary Science Reviews* 189, 31–42.

Haslett, J., Parnell, A.C., 2008. A simple monotone process with application to radiocarbon-dated depth chronologies. *Journal of the Royal Statistical Society: Series C* (*Applied Statistics*) 57(4), 399–418.

Herzschuh, U., 2006. Palaeo-moisture evolution in monsoonal Central Asia during the last 50,000 years. *Quaternary Science Reviews* 25, 163–178.

Hodell, D.A., Schelske, C.L., 1998. Production, sedimentation, and isotopic composition of organic matter in Lake Ontario. *Limnology and Oceanography* 43, 200–214.

Jin, Z., Cao, J., Wu, J., Wang, S., 2006. A Rb/Sr record of catchment weathering response to Holocene climate change in Inner Mongolia. *Earth Surface Processes and Landforms* 31, 285–291.

Ju, J., Zhu, L., Feng, J.-L., Wang, J., Wang, Y., Xie, M., Peng, P., Zhen, X., Lü, X., 2012. Hydrodynamic process of Tibetan Plateau lake revealed by grain size: Case study of Pumayum Co. *Chinese Science Bulletin* 57, 2433–2441.

Juyal, N., 2014. Ladakh: the high-altitude Indian cold desert. In *Landscapes and Landforms of India*. Springer, Dordrecht, 115–124.

Kale, V.S., Mishra, S., Baker, V.R., 2003. Sedimentary records of palaeofloods in the bedrock gorges of the Tapi and Narmada Rivers, central India. *Current Science* 84, 1072–1079.

Kale, V.S., Singhvi, A.K., Mishra, P.K., Banerjee, D., 2000. Sedimentary records and luminescence chronology of Late Holocene palaeofloods in the Luni River, Thar Desert, northwest India. *Catena* 40, 337–358.

Kaniewski, D., Van Campo, E., 2017. 3.2 Ka BP Megadrought and the Late Bronze Age Collapse. In Weiss, H. (Ed.), *Megadrought and Collapse: From Early Agriculture to Angkor*. Oxford University Press, New York, pp. 161–182.

Kar, R., Ranhotra, P.S., Bhattacharyya, A., Sekar B., 2002. Vegetation vis-á-vis climate and glacial fluctuations of the Gangotri glacier since the last 2000 years. *Current Science* 82, 347–351.

Kathayat, G., Cheng, H., Sinha, A., Yi, L., Li, X., Zhang, H., Li, H., Ning, Y., Edwards, R.L. 2017. The Indian monsoon variability and civilization changes in the Indian subcontinent. *Science Advances* 3, e1701296.

https://doi.org/10.1017/qua.2020.22 Published online by Cambridge University Press

Kaufman, D.S., Schneider, D.P., McKay, N.P., Ammann, C.M., Bradley, R.S., Briffa, K.R., Miller, G.H., *et al*., 2009. Recent warming reverses long-term Arctic cooling. *Science* 325, 1236–1239.

Kohn, M.J., 2010. Carbon isotope compositions of terrestrial C3 plants as indicators of (paleo)ecology and (paleo)climate. *Proceedings of the National Academy of Sciences of the United States of America* 107, 19691–9695.

Kohn, M.J., 2016. Carbon isotope discrimination in C3 land plants is independent of natural variations in p_{CO2}. *Geophysical Perspective Letters* 2, 35–43.

Kotlia, B.S., Joshi, L.M., 2013. Late Holocene climatic changes in Garhwal Himalaya. *Current Science* 104 911–919.

Kotlia, B.S., Singh, A.K., Joshi, L.M., Dhaila, B.S., 2015. Precipitation variability in the Indian Central Himalaya during last ca. 4,000 years inferred from a speleothem record: Impact of Indian Summer Monsoon (ISM) and Westerlies. *Quaternary International* 371, 244–253.

Kulke, H., Rothermund, D., 2004. *A History of India*. Psychology Press, London.

Kumar, K., Agrawal, S., Sharma, A., Pandey, S., 2019. Indian summer monsoon variability and vegetation changes in the core monsoon zone, India, during the Holocene: A multiproxy study. *The Holocene* 1, 110–119. doi: 10.1177/0959683618804641

Kumar, K.R., Kumar, K.K., Pant, G.B., 1994. Diurnal asymmetry of surface temperature trends over India. *Geophysical Research Letters* 21 677–680.

Lamb, H.H., 1965. The early medieval warm epoch and its sequel. *Palaeogeography Palaeoclimatology, Palaeoecology* 1, 13–37.

Lee, S.Y., Seong, Y.B., Owen, L.A., Murari, M.K., Lim, H.S., Yoon, H.I., Yoo, K.-C., 2014. Late Quaternary glaciation in the Nun-Kun massif, northwestern India. *Boreas* 43, 67–89.

Lehner, F., Born, A., Raible, C.C., Stocker, T.F., 2013. Amplified inception of European Little Ice Age by sea ice–ocean–atmosphere feedbacks. *Journal of Climate* 26, 7586–7602.

Leipe, C., Demske, D., Tarasov, P. 2014. A Holocene pollen record from the northwestern Himalayan lake Tso Moriri: Implications for palaeoclimatic and archaeological research. *Quaternary International* 348, 93–112.

Leipe, C., Demske, D., Tarasov, P.E., Wünnemann, B., Riedel, F., HIMPAC Members, 2014. Potential of pollen and non-pollen palynomorph records from Tso Moriri (Trans-Himalaya, NW India) for reconstructing Holocene limnology and human–environmental interactions. *Quaternary International* 348, 113–129.

Ljungqvist, F.C., 2010. A new reconstruction of temperature variability in the extra-tropical Northern Hemisphere during the last two millennia. *Geografiska Annaler: Series A, Physical Geography* 92, 339–351.

Maizels, J.K., 1977. Experiments on the origin of kettle-holes. *Journal of Glaciology,* 18, 291–303.

Mann, M.E., Zhang, Z., Rutherford, S., Bradley, R.S., Hughes, M.K., Shindell, D., Ammann, C., Faluvegi, G., Ni, F., 2009. Global signatures and dynamical origins of the Little Ice Age and Medieval Climate Anomaly. *Science* 326, 1256–1260.

Martin-Puertas, C., Matthes, K., Brauer, A., Muscheler, R., Hansen, F., Petrick, C., Aldahan, A., Possnert, G., Van Geel, B., 2012. Regional atmospheric circulation shifts induced by a grand solar minimum. *Nature Geoscience* 5, 397–401.

Mayewski, P.A., Lyons, W.B., Ahmad, N., Smith, G., Pourchet, M., 1984. Interpretation of the chemical and physical time-series retrieved from Sentik Glacier, Ladakh Himalaya, India. *Journal of Glaciology* 30, 66–76.

Mazari, R.K., Bagati, T.N., Chauhan, M.S., Rajagopalan, G., 1996. Paleoclimatic record of last 2000 years in Trans-Himalayan Lahaul-Spiti region. In: Mikami, T., Matsumoto, E., Ohta, S., Sweda, T. (Eds.), *Proceedings of Paleoclimate and Environmental Variability in Austral-Asian Transect during the Past 2000 Years: Proceedings of the 1995 Nagoya IGBP-PAGES/PEPII Symposium*. Nagoya, Japan, 262–269.

McGregor, H.V., Evans, M.N., Goosse, H., Leduc, G., Martrat, B., Addison, J.A., Mortyn, P.G., *et al*., 2015. Robust global ocean cooling trend for the pre-industrial Common Era. *Nature Geoscience* 8, 671–678.

Meyers, P.A., Lallier-Vergés, E., 1999. Lacustrine sedimentary organic matter records of late Quaternary paleoclimates. *Journal of Paleolimnology* 21, 345–372.

Miller, G.H., Geirsdóttir, Á., Zhong, Y., Larsen, D.J., Otto-Bliesner, B.L., Holland, M.M., Bailey, D.A., *et al*., 2012. Abrupt onset of the Little Ice Age triggered by volcanism and sustained by sea-ice/ocean feedbacks. *Geophysical Research Letters* 39, L02708.

Mishra, A., 2017. Changing Temperature and Rainfall Patterns of Uttarakhand. *International Journal of Environmental Sciences and Natural Resources* 7, 1–6.

Mishra, P.K., Prasad, S., Ambili, A., Plessen, B., Jehangir, A., Gaye, B., Menzel, P., Weise, S.M., Yousuf, A.R., 2015. Carbonate isotopes from high altitude Tso Moriri Lake (NW Himalayas) provide clues to late glacial and Holocene moisture source and atmospheric circulation changes. *Palaeogeography, Palaeoclimatology, Palaeoecology* 425, 76–83.

Misra, P., Tandon, S.K., Sinha, R., 2019. Holocene climate records from lake sediments in India: Assessment of coherence across climate zones. *Earth-Science Reviews* 190, 370–397.

Moros, M., Emeis, K., Risebrobakken, B., Snowball, I., Kuijpers, A., McManus, J., Jansen, E., 2004. Sea surface temperatures and ice rafting in the Holocene North Atlantic: climate influences on northern Europe and Greenland. *Quaternary Science Reviews* 23, 2113–2126.

Murari, M.K., Owen, L.A., Dortch, J.M., Caffee, M.W., Dietsch, C., Fuchs, M., Haneberg, W.C., Sharma, M.C. and Townsend-Small, A., 2014. Timing and climatic drivers for glaciation across monsoon-influenced regions of the Himalayan–Tibetan orogen. *Quaternary Science Reviews* 88, 159–182.

National Research Council 2005. The Geological Record of Ecological Dynamics—Understanding the Biotic Effects of Future Environmental Change. National Academies Press, Washington, DC.

Neff, U., Burns, S.J., Mangini, A., Mudelsee, M., Fleitmann, D., Matter, A., 2001. Strong coherence between solar variability and the monsoon in Oman between 9 and 6 kyr ago. *Nature* 411, 290–293.

Oksanen, J., Blanchet, F.G., Friendly, M., Kindt, R., Legendre, P., McGlinn, D., Minchin, P.R., *et al*., 2019. vegan: Community Ecology Package. R package version 2.5-5. https://CRAN.R-project.org/package=vegan

Overpeck, J., Anderson, D., Trumbore, S., Prell, W., 1996. The southwest Indian Monsoon over the last 18 000 years. *Climate Dynamics* 12, 213–225.

Owen, L.A., Derbyshire, E., Richardson, S., Benn, D.I., Evans, D.J.A., Mitchell, W.A., 1996. The quaternary glacial history of the Lahul Himalaya, northern India. *Journal of Quaternary Science* 11, 25–42.

Owen, L.A., Dortch, J.M., 2014. Nature and timing of Quaternary glaciation in the Himalayan–Tibetan orogen. *Quaternary Science Reviews*, 88, 14–54.

https://doi.org/10.1017/qua.2020.22 Published online by Cambridge University Press

Park, J., Park, J., Yi, S., Kim, J.C., Lee, E., Choi, J., 2019. Abrupt Holocene climate shifts in coastal East Asia, including the 8.2 ka, 4.2 ka, and 2.8 ka BP events, and societal responses on the Korean peninsula. *Scientific Reports* 9, 10806. doi:10.1038/s41598-019-47264-8.

Parnell, A., 2016. Bchron: Radiocarbon dating, age-depth modelling, relative sea level rate estimation, and non-parametric phase modelling. R package version 4.1.1.http://CRAN.R-project.org/package=Bchron.

Patnaik, R., Gupta, A.K., Naidu, P.D., Yadav, R.R., Bhattacharyya, A., Kumar, M., 2012. Indian monsoon variability at different time scales: Marine and terrestrial proxy records. *Proceedings of the Indian National Science Academy* 78, 535–547

Petit, J.R., Jouzel, J., Raynaud, D., Barkov, N.I., Barnola, J.-M., Basile, I., Bender, M., *et al*., 1999. Climate and atmospheric history of the past 420,000 years from the Vostok ice core, Antarctica. *Nature* 399, 429.

Petrie C.A., Singh R.N., Bates J., Dixit Y., French C.A.I., Hodell D.A., Jones P.J., *et al*., 2017. Adaptation to variable environments, resilience to climate change: Investigating Land, Water and Settlement in Indus Northwest India. *Current Anthropology* 58, 1–30.

Phadtare, N.R., 2000. Sharp decrease in summer monsoon strength 4000–3500 cal. yr B.P. in the central higher Himalaya of India based on pollen evidence from alpine peat. *Quaternary Research* 53, 122–129.

Polanski, S., Fallah, B., Befort, D.J., Prasad, S., Cubasch, U., 2014. Regional moisture change over India during the past millennium: A comparison of multi-proxy reconstructions and climate model simulations. *Global and Planetary Change* 122, 176–185.

Prasad, S., Ambili, A., Riedel, N., Sarkar, S., Menzel, P., Basavaiah, N., Krishnan, R., *et al*., 2014. Prolonged monsoon droughts and links to Indo-Pacific warm pool: A Holocene record from Lonar Lake, central India. *Earth and Planetary Science Letters* 391, 171–182.

Prasad, S., Enzel, Y., 2006. Holocene paleoclimates of India. *Quaternary Research* 66, 442–453.

Prasad, V., Farooqui, A., Sharma, A., Phartiyal, B., Chakraborty, S., Bhandari, S., Raj, R., Singh, A., 2014. Mid–late Holocene monsoonal variations from mainland Gujarat, India: A multi-proxy study for evaluating climate culture relationship. *Palaeogeography, Palaeoclimatology, Palaeoecology* 397, 38–51.

Quade, J., Cater, J.M.L., Ojha, T.P., Adam, J., Harrison, T.M., 1995, Late Miocene environmental change in Nepal and the northern Indian subcontinent:Stable isotopic evidence from paleosols. *Geological Society of America Bulletin* 107, 1381–1397

Quade, J., Cerling, T.E., Bowman, J.R., 1989. Development of Asian monsoon revealed by marked ecologic shift in the latest Miocene of northern Pakistan: *Nature* 342, 163–166.

Ranhotra, P.S., Bhattacharyya, A., Kar, R., Sekar, B., 2001. Vegetation and climatic changes around Gangotri glacier during Holocene. *Geological Survey of India Special Publication* 65, 67–71.

Rao, Z., Guo, W., Cao, J., Shi, F., Jiang, H., Li, C., 2017. Relationship between the stable carbon isotopic composition of modern plants and surface soils and climate: A global review. *Earth-Science Reviews* 165, 110–119.

Rao, Z., Xu, Y., Xia, D.S., Xie, L., Chen, F., 2013. Variation and paleoclimatic significance of organic carbon isotopes of Ili loess in arid Central Asia. *Organic Geochemistry* 63, 56–63.

Ratnagar, S., 2002. *The End of the Great Harappan Tradition*. Manohar Publishers and Distributors, New Delhi, India.

Rawat, S., Gupta, A.K., Sangode, S.J., Srivastava, P., Nainwal, H.C., 2015. Late Pleistocene–Holocene vegetation and Indian summer monsoon record from the Lahaul, Northwest Himalaya, India. *Quaternary Science Reviews* 114, 167–181.

R Core Team, 2019. R: A Language and Environment for Statistical Computing. R Foundation for Statistical Computing, Vienna, Austria. https://www.R-project.org/.

Reimer, P.J., Bard, E., Bayliss, A., Beck, J.W., Blackwell, P.G., Ramsey, C.B., Buck, C.E., *et al*., 2013. IntCal13 and Marine13 radiocarbon age calibration curves 0–50,000 years cal BP. *Radiocarbon* 55, 1869–1887.

Robinson, Z., 2010. The hydrological and geomorphological evolution of kettle-hole lakes, Skeiðarársandur, SE Iceland. *Geophysical Research Abstracts* 12, EGU2010-12456-1.

Rowan, A.V., 2017. The 'Little Ice Age' in the Himalaya: A review of glacier advance driven by Northern Hemisphere temperature change. *The Holocene* 27(2), 292–308.

Rühland, K., Phadtare, N.R., Pant, R.K., Sangode, S.J., Smol, J.P., 2006. Accelerated melting of Himalayan snow and ice triggers pronounced changes in a valley peatland from northern India. *Geophysical Research Letters* 33, L15709.

Rupper, S., Roe, G., Gillespie, A., 2009. Spatial patterns of Holocene glacier advance and retreat in Central Asia. *Quaternary Research* 72, 337–346.

Sanwal, J., Kotlia, B.S., Rajendran, C., Ahmad, S.M., Rajendran, K., Sandiford, M., 2013. Climatic variability in Central Indian Himalaya during the last ~1800 years: Evidence from a high resolution speleothem record. *Quaternary International* 304, 183–192.

Sarkar, S., Prasad, S., Wilkes, H., Riedel, N., Stebich, M., Basavaiah, N., Sachse, D., 2015. Monsoon source shifts during the drying mid-Holocene: Biomarker isotope based evidence from the core 'monsoon zone' (CMZ) of India. *Quaternary Science Reviews* 123, 144–157.

Searle, M.P., Fryer, B.J., 1986. Garnet, tourmaline and muscovite-bearing leucogranites, gneisses, and migmatites of the Higher Himalayas from Zanskar, Kulu, Lahoul and Kashmir. *Geological Society, London, Special Publications* 19, 85–201.

Sharma, A., Kumar, K., Laskar, A., Singh, S.K., Mehta, P., 2017. Oxygen, deuterium, and strontium isotope characteristics of the Indus River water system. *Geomorphology* 284, 5–16.

Sharma, A., Phartiyal, B., 2018. Late Quaternary Palaeoclimate and Contemporary Moisture Source to Extreme NW India: A Review on Present Understanding and Future Perspectives. *Frontiers in Earth Science* 6, 150. doi: 10.3389/feart.2018.00150.

Sharma, C., Chauhan, M.S., 2001. Late Holocene vegetation and climate of Kupur (Sikkim), eastern Himalaya, India. *Journal of the Palaeontological Society of India* 46, 51–58.

Sharma, S., Hussain, A., Mishra, A.K., Lone, A., Solanki, T., Khan, M.K., 2018. Geomorphic investigation of the late-Quaternary landforms in the southern Zanskar Valley, NW Himalaya. *Journal of Earth System Science* 127, 9. doi.org/10.1007/s12040-017-0911-2

Sharma, S., Shukla, A.D., 2018. Factors governing the pattern of glacier advances since the Last Glacial Maxima in the transitional climate zone of the Southern Zanskar Ranges, NW Himalaya. *Quaternary Science Reviews* 201, 223–240.

Shekhar, M., Bhardwaj, A., Singh, S., Ranhotra, P.S., Bhattacharyya, A., Pal, A.K., Roy, I., Martín-Torres, F.J., Zorzano, M.P., 2017. Himalayan glaciers experienced significant mass loss during later phases of little ice age. *Scientific Reports* 7, 10305.

Shrestha, A.B., Wake, C.P., Mayewski, P.A., Dibb, J.E., 1999. Maximum temperature trends in the Himalaya and its vicinity: An analysis based on temperature records from Nepal for the period 1971–94. *Journal of Climate* 12, 2775–2786.

https://doi.org/10.1017/qua.2020.22 Published online by Cambridge University Press

Sinha, A., Berkelhammer, M., Stott, L., Mudelsee, M., Cheng, H., Biswas, J., 2011. The leading mode of Indian Summer Monsoon precipitation variability during the last millennium. *Geophysical Research Letters* 38, 532–560.

Sinha, A., Cannariato, K.G., Stott, L.D., Cheng, H., Edwards, R.L., Yadava, M.G., Ramesh, R., Singh, I.B., 2007. A 900-year (600 to 1500 AD) record of the Indian summer monsoon precipitation from the core monsoon zone of India. *Geophysical Research Letters* 34 L16707. doi:10.1029/2007GL030431.

Sinha, A., Kathayat, G., Cheng, H., Breitenbach, S.F., Berkelhammer, M., Mudelsee, M., Biswas, J., Edwards, R.L., 2015.Trends and oscillations in the Indian summer monsoon rainfall over the last two millennia. *Nature Communications* 6, 6309.

Smol, J.P., 2002. Pollution of Lakes and Rivers—APaleoenvironmental Perspective. Arnold, London.

Srivastava, P., Agnihotri, R., Sharma, D., Meena, N., Sundriyal, Y.P., Saxena, A., Bhushan, R., *et al*., 2018. 8000-year monsoonal record from Himalaya revealing reinforcement of tropical and global climate systems since mid-Holocene. *Scientific Reports* 7, 14515. doi:10.1038/s41598-017-15143-9.

Staubwasser, M., Sirocko, F., Grootes, P.M., Segl, M., 2003. Climate change at the 4.2 ka BP termination of the Indus valley civilization and Holocene south Asian monsoon variability. *Geophysical Research Letters* 30, 1425. doi:10.1029/2002GL016822.

Steinhilber, F., Beer, J., Fröhlich, C., 2009. Total solar irradiance during the Holocene. *Geophysical Research Letters* 36, L19704, doi:10.1029/2009GL040142.

Sternberg, L., Deniro, M.J., Ajie, H., 1984. Stable hydrogen isotope ratios of saponifiable lipids and cellulose nitrate from CAM, C_3 and C_4 plants. *Phytochemistry* 23, 2475–2477.

Svendsen, J.I., Mangerud, J., 1997. Holocene glacial and climatic variations on Spitsbergen, Svalbard. *The Holocene* 7, 45–57.

Thomas, E.R., Wolff, E.W., Mulvaney, R., Steffensen, J.P., Johnsen, S.J., Arrowsmith, C., White, J.W., Vaughn, B.H., Popp, T., 2007. The 8.2 ka event from Greenland ice cores. *Quaternary Science Reviews* 26, 70–81.

Thompson, L.G., Yao, T., Davis, M.E., Henderson, K.A., Mosley-Thompson, E., Lin, P.N., Beer, J., Synal, H.A., Cole-Dai, J., Bolzan, J.F., 1997. Tropical climate instability: the last glacial cycle from a Qinghaie Tibetan ice core. *Science* 276, 1821–1825.

Trenberth, K.E., Dai, A., Rasmussen, R.M., Parsons, D.B., 2003. The changing character of precipitation. *Bulletin of the American Meteorological Society* 84, 1205–1217.

Von Rad, U., Schaaf, M., Michels, K.H., Schulz, H., Berger, W.H., Sirocko, F., 1999. A 5000-yr record of climate change in varved sediments from the Oxygen Minimum Zone off Pakistan, Northeastern Arabian Sea. *Quaternary Research* 51, 39–53.

Wang, B., Wu, R., Lau, W.K.M., 2001. Interannual variability of the Asian summer monsoon: Contrasts between the Indian and the western North Pacific–East Asian monsoons. *Journal of Climate* 14, 4073–4090.

Wang, Y., Cheng, H., Edwards, R.L., He, Y., Kong, X., An, Z., Wu, J., Kelly, M.J., Dykoski, C.A., Li, X., 2005. The Holocene Asian monsoon: Links to solar changes and North Atlantic climate. *Science* 308, 854–857.

Wanner, H., Beer, J., Bütikofer, J., Crowley, T.J., Cubasch, U., Flückiger, J., Goosse, H., Grosjean, M., *et al*., 2008. Mid-to Late Holocene climate change: an overview. *Quaternary Science Reviews* 27, 1791–1828.

Warrier, A.K., Pednekar, H., Mahesh, B.S., Mohan, R., Gazi, S., 2016. Sediment grain size and surface textural observations of quartz grains in late quaternary lacustrine sediments from Schirmacher Oasis, East Antarctica: Paleoenvironmental significance. *Polar Science* 10, 89–100.

Wiersma, A.P., Renssen, H., 2006. Model-data comparison for the 8.2 ka B.P. event: confirmation of a forcing mechanism by catastrophic drainage of Laurentide Lakes. *Quaternary Science Reviews* 25, 63–88.

Witzel, M., 1987. On the Localisation of Vedic Texts and Schools (Materials on Vedic Sakhas, 7), in India and the Ancient World. History, Trade and Culture before A.D. 650. P.H.L. Eggermont Jubilee Volume, ed. by G. Pollet, Orientalia Lovaniensia Analecta 25, Leuven 1987, 173–213.

Witzel, M., 1999. Aryan and Non-Aryan Names in Vedic India. Data for the Linguistic Situation, c. 1900–500 B.C., in J. Bronkhorst and M. Deshpande, eds., *Aryans and Non-Non-Aryans, Evidence*, Interpretation, and Ideology, Cambridge (Harvard Orienatal Series, Opera Minora 3), 337–404.

Wright, R.P., 2010. The Ancient Indus: Urbanism, Economy, and Society in South Asia.Cambridge University Press.

Wünnemann, B., Demske, D., Tarasov, P., Kotlia, B.S., Reinhardt-Imjela, C., Bloemendal, J., Diekmann, B., *et al*., 2010. Hydrological evolution during the last 15 kyr in the Tso Kar Lake basin (Ladakh, India), derived from geomorphological, sedimentological and palynological records. *Quaternary Science Reviews* 29, 1138–1155.

Xu, C., Sano, M., Dimri, A.P., Ramesh, R., Nakatsuka, T., Shi, F., Guo, Z., 2018. Decreasing Indian summer monsoon on the northern Indian sub-continent during the last 180 years: evidence from five tree-ring cellulose oxygen isotope chronologies. *Climate of the Past* 14, 653–664.

Yadava, M.G., Ramesh, R., 2001. Past rainfall and trace element variations in a tropical speleothem from India. *Mausam* 52, 307–316.

Yadav, R.R., Braeuning, A., Singh, J., 2011. Tree ring inferred summer temperature variations over the last millennium in western Himalaya, India. *Climate Dynamics* 36, 1545–1554.

Yang, X., Zhu, B., Wang, X., Li, C., Zhou, Z., Chen, J., Yin, J., Lu, Y., 2008. Late Quaternary environmental changes and organic carbon density in the Hunshandake Sandy Land, eastern Inner Mongolia, China. *Global and Planetary Change,* 61, 70–78.

Yanhong, W., Lücke, A., Zhangdong, J., Sumin, W., Schleser, G.H., Battarbee, R.W., Weilan, X., 2006. Holocene climate development on the central Tibetan Plateau: A sedimentary record from Cuoe Lake. *Palaeogeography, Palaeoclimatology, Palaeoecology* 234, 328–340.

Yuan, S., 2009. *The Mystery of the Guge Kingdom in Tibet*. China Religious Culture Publisher, China.

Zhu, H., Zheng, Y., Shao, X., Liu, X., Xu, Y., Liang, E., 2008. Millennial temperature reconstruction based on tree-ring widths of Qilian juniper from Wulan, Qinghai Province, China. *Chinese Science Bulletin* 53, 3914–3920.

https://doi.org/10.1017/qua.2020.22 Published online by Cambridge University Press